

Control of Sleep Onset by Shal/K_v4 Channels in *Drosophila* Circadian Neurons

Ge Feng,^{1,2} Jiaying Zhang,¹ Minzhe Li,¹ Lingzhan Shao,¹ Luna Yang,¹ Qian Song,¹ and  Yong Ping^{1,2}

¹Bio-X Institutes, Key laboratory for the Genetics of Developmental and Neuropsychiatric Disorders, Ministry of Education, Shanghai Jiao Tong University, Shanghai 200240, China, and ²Shanghai Key Laboratory of Psychotic Disorders (No.13dz2260500), Shanghai Mental Health Center, School of Medicine, Shanghai Jiao Tong University, Shanghai 200030, China

Sleep is highly conserved across animal species. Both wake- and sleep-promoting neurons are implicated in the regulation of wake–sleep transition at dusk in *Drosophila*. However, little is known about how they cooperate and whether they act via different mechanisms. Here, we demonstrated that in female *Drosophila*, sleep onset was specifically delayed by blocking the Shaker cognate L channels [Shal; also known as voltage-gated K⁺ channel 4 (K_v4)] in wake-promoting cells, including large ventral lateral neurons (l-LNvs) and pars intercerebralis (PI), but not in sleep-promoting dorsal neurons (DN1s). Delayed sleep onset was also observed in males by blocking K_v4 activity in wake-promoting neurons. Electrophysiological recordings show that K_v4 channels contribute A-type currents in LNvs and PI cells, but are much less conspicuous in DN1s. Interestingly, blocking K_v4 in wake-promoting neurons preferentially increased firing rates at dusk ~ZT13, when the resting membrane potentials and firing rates were at lower levels. Furthermore, pigment-dispersing factor (PDF) is essential for the regulation of sleep onset by K_v4 in l-LNvs, and downregulation of PDF receptor (PDFR) in PI neurons advanced sleep onset, indicating K_v4 controls sleep onset via regulating PDF/PDFR signaling in wake-promoting neurons. We propose that K_v4 acts as a sleep onset controller by suppressing membrane excitability in a clock-dependent manner to balance the wake–sleep transition at dusk. Our results have important implications for the understanding and treatment of sleep disorders such as insomnia.

Key words: circadian; *Drosophila*; Kv4; Shaker; sleep

Significance Statement

The mechanisms by which our brains reversibly switch from waking to sleep state remain an unanswered and intriguing question in biological research. In this study, we identified that Shal/K_v4, a well known voltage-gated K⁺ channel, acts as a controller of wake–sleep transition at dusk in *Drosophila* circadian neurons. We find that interference of K_v4 function with a dominant-negative form (DNK_v4) in subsets of circadian neurons specifically disrupts sleep onset at dusk, although K_v4 itself does not exhibit circadian oscillation. K_v4 preferentially downregulates neuronal firings at ZT9–ZT17, supporting that it plays an essential role in wake–sleep transition at dusk. Our findings may help understand and eventually treat sleep disorders such as insomnia.

Introduction

Sleep is an essential process that is believed to be regulated by circadian clock and other factors. *Drosophila melanogaster* has

become an ideal and well accepted model for sleep and circadian rhythms research (Kayser and Biron, 2016; Dubowy and Sehgal, 2017). In *Drosophila*, groups of neurons that regulate sleep were found in mushroom body neurons (MBNs), fan-shaped body (FB), the ellipsoid body (EB), pars intercerebralis (PI), large ventral lateral neurons (l-LNvs), dorsal neurons (DN1s), pars lateralis, and dorsolateral neurons (LNds; Strauss and Heisenberg, 1993; Joiner et al., 2006; Pitman et al., 2006; Foltényi et al., 2007; Shang et al., 2008; Sheeba et al., 2008a; Keene et al., 2010; Afonso et al., 2015; Artiushin and Sehgal, 2017). Among them, l-LNvs are a group of wake-promoting neurons, which express neuropeptide pigment-dispersing factor (PDF), and regulate night-time sleep (Parisky et al., 2008). PDF, released by LNvs (also named PDF neurons), regulates circadian and sleep by acting on PDF receptor (PDFR)-expressing neurons, including LNds, DN1s,

Received March 25, 2018; revised Aug. 25, 2018; accepted Aug. 29, 2018.

Author contributions: G.F. and Y.P. wrote the first draft of the paper; G.F., J.Z., and Y.P. edited the paper; G.F., Q.S., and Y.P. designed research; G.F., J.Z., M.L., L.S., L.Y., Q.S., and Y.P. performed research; G.F. and Y.P. contributed unpublished reagents/analytic tools; G.F., M.L., Q.S., and Y.P. analyzed data; G.F., Q.S., and Y.P. wrote the paper.

This work was supported by a National Natural Science Foundation of China Grant (81371482), a National Science and Technology Ministry Major Project Grant (2016YFC0906400), and a Science and Technology Commission of Shanghai Municipality Grant (18ZR1419400). We thank Hai Huang, Bingwei Lu, and Xiong-Li Yang for critical reading of the paper and helpful feedback.

The authors declare no competing financial interests.

Correspondence should be addressed to Dr. Yong Ping, Bio-X Institutes at SJTU, 800 Dongchuan Road, Shanghai 200240. E-mail: yoping@sjtu.edu.cn.

DOI:10.1523/JNEUROSCI.0777-18.2018

Copyright © 2018 the authors 0270-6474/18/389059-13\$15.00/0

and PI neurons (Im and Taghert, 2010; Dubowy and Sehgal, 2017). DN1s, a group of potent sleep-promoting neurons at dusk, show effect on transition from wake to sleep via feedback mechanisms and may also relay signals from PDF neurons to PI (Cavanaugh et al., 2014; Kunst et al., 2014; Guo et al., 2016). PI, analogous to the mammalian hypothalamus, is an important output brain region for rest–activity rhythms (Foltenyi et al., 2007; Cavanaugh et al., 2014; Park et al., 2014; Cavey et al., 2016), and activation of PI neurons reduced sleep amount (Crocker et al., 2010). Although previous studies have implicated various types of circadian neurons in regulating sleep behavior, it remains to be determined whether these sleep- and wake-promoting neurons control wake/sleep amount and transition via different mechanisms, and the precise mechanisms by which they cooperate in the brain.

Insomnia is a condition characterized by difficulty initiating or maintaining sleep and dissatisfaction with sleep quantity or quality (Rosenberg, 2006). Although the biological basis of classification of initiating and maintaining sleep is unknown, sleep initiation is suggested to be uncoupled from sleep maintenance in *Drosophila*. In particular, hyperactivity of l-LNVs resulted in increased sleep latency and GABA_A receptor played a critical role in the regulation (Agosto et al., 2008; Chung et al., 2009; Liu et al., 2014; Li et al., 2017). Another study shows that sleep initiation is dependent on the *amnesiac* gene expression (Liu et al., 2008). However, our understanding of the key molecules and neurons that control wake–sleep transition remains rudimentary.

Compared with wake state, there are large-scale changes in neuronal activity during sleep. Reports have shown that different types of ion channels, including Shaker and sandman, are required for normal wake–sleep cycles (Cirelli et al., 2005; Pimentel et al., 2016). Only two genes, *Shaker/K_v1* and *Shal/K_v4*, encode voltage-gated A-type K⁺ channels in *Drosophila* neurons, whereas mammals contain multiple genes (Salkoff and Wyman, 1981; Wei et al., 1990; Covarrubias et al., 1991). In most *Drosophila* neurons, Shaker expression is extensively restricted to axons and terminals (Rogerio et al., 1997; Ueda and Wu, 2006). In contrast, K_v4 channels are localized exclusively to soma and dendrites (Gasque et al., 2005; Bergquist et al., 2010; Diao et al., 2010; Srinivasan et al., 2012). In mammals, neurons in suprachiasmatic nucleus (SCN) function as central pacemaker and their firing activity exhibits circadian oscillation (Colwell, 2011). Loss of Shaker results in dysregulated sleep patterns in both *Drosophila* and mammals, and most K_v channels contributing to A-type currents (*I_A*) regulate activity of neurons in SCN (Cirelli et al., 2005; Douglas et al., 2007; Granados-Fuentes et al., 2012). However, little is known about the role of K_v4 playing in sleep.

In this study, we found that *Shal*⁴⁹⁵ mutants exhibited delayed sleep onset at dusk, which could be rescued by restoring *Shal/K_v4* expression. Our results further demonstrated that K_v4 controls sleep onset in wake-promoting neurons, but not in subsets of sleep-promoting neurons. These results support that K_v4 has an important role in controlling wake–sleep transition.

Materials and Methods

Animals. Flies were kept at 23°C on cornmeal, yeast, and sucrose and agar food. *w¹¹¹⁸* (5905; RRID:BDSC_5905), *elav-GAL4* (458; RRID:BDSC_8760), *pdf-GAL4* (6900, 6899; RRIDs:BDSC_69002, BDSC_6899), *50y-GAL4* (30820; RRID:BDSC_30820), *tub-GAL80^{ts}* (7019), *UAS-dTrpA1* (26263), *pdf⁰¹* (26654; RRID:BDSC_26654), *Sh^{trms}* (22837), *UAS-EKO* (40973; RRID:BDSC_40974), *UAS-Shal-RNAi* (31879), and *clk4.1M-GAL4* (36316; RRID:BDSC_36316) were obtained from the Bloomington Stock Center. *UAS-CD8GFP* (RRID:BDSC_5137), *Shal⁴⁹⁵*

(Bergquist et al., 2010), *R18H11-GAL4* (RRID:BDSC_48832), *UAS-white-RNAi*, and *pdf-GAL80* (Stoleru et al., 2004) were obtained from Drs. Susan Tsunoda, Bingwei Lu, and Yufeng Pan. *UAS-DNK_v4* and *UAS-K_v4* transgenic lines were generated previously (Ping and Tsunoda, 2011; Ping et al., 2011). Flies were outcrossed for more than five generations with the *w¹¹¹⁸* strain to standardize the background.

Sleep and activity assays. All behavior was done on female flies unless otherwise specified. Three- to 5-d-old virgin flies were monitored at 25°C in glass tube containing 5% sucrose and 2% agar using the Drosophila Activity Monitoring System (Trikinetics). Flies were raised in behavior tubes for >72 h at 25°C in 12 h light/dark (LD) conditions for acclimation before data collection. Flies were entrained at least 3 d in LD before switching to constant darkness (DD). Activity counts were collected in 1 min bins in LD for 3 d. Sleep was defined as 5 consecutive minutes of inactivity. Sleep latency was measured from the time lights-off to the onset of first sleep episode. Sleep parameters were analyzed using R software. For analysis of sleep in DD, sleep latency was calculated from CT12. For *UAS-dTrpA1* experiments, data were recorded at 29°C to activate the relevant neurons. For conditional expression experiments using *Tub-GAL80^{ts}*, animals containing *UAS-DNK_v4*, driven by *Tub-GAL80^{ts}* and *PDF-GAL4*, were reared at 18°C to prevent DNK_v4 expression at developmental stages. The temperature was then raised to 29°C to induce expression for 14 d post-eclosion, followed by conventional sleep assays. Free-running activity was measured over 3 d entrainment for LD and over 7 d for DD, as reported previously (Song et al., 2017). Rhythmic flies were defined by χ^2 periodogram analysis (ClockLab software), and power is a measure of rhythm amplitude and corresponds to the height of the periodogram peak above the significance line. More than 20 flies were examined for each genotype and condition, and dead flies were excluded from the data analysis.

Electrophysiology. Flies were kept at 25°C in LD cycles. Whole-cell recordings were performed in perforated patch-clamp configuration by adding 400–800 μ g/ml amphotericin-B (Sigma-Aldrich) in the pipette, as reported previously (Feng et al., 2018). For voltage-dependent K⁺ current recordings from GFP-labeled PDF (l-LNVs), DN1s, and PI neurons in the isolated brain, we first dissected brain in the *Drosophila* culture medium (Invitrogen) and then we exchanged culture medium to the recording external solution (in mM): 110 NaCl, 2 KCl, 6 MgCl₂, 1 CaCl₂, 5 glucose, 20 NaHCO₃, 2 NaH₂PO₄. Solution was continuously bubbled with carbogen (5% oxygen and 95% carbon dioxide) throughout recording, pH was set at 7.2. TTX (1 μ M) and nifedipine (10 μ M) were added to the external solution to block Na⁺ and Ca²⁺ currents (for *I_A* recordings). Electrodes were filled with internal solution (in mM): K-gluconate, 120; KCl, 20; Mg-ATP, 4; Na-GTP, 0.5; HEPES, 10; EGTA, 1.1; MgCl₂, 2; CaCl₂, 0.1, with pH 7.2. The l-LNVs were distinguished from the sLNVs by their size and anatomical location. We performed all recordings at room temperature. Electrode resistances for all recordings were 5–10 M Ω . Gigaohm seals were obtained for whole-cell recordings. Cells were clamped at –80 mV. The K_v2–K_v3-mediated delayed rectifier (DR) component was recorded using a pre-pulse of –45 mV to completely inactivate K_v4 channels, before stepping to a test potential of +50 mV; the K_v4 current or *I_A* was then isolated by subtracting this DR component from the total whole-cell current elicited from a pre-pulse of –125 mV, stepping to a test potential of +50 mV. In current-clamp experiments, we clamped the membrane current at 0 pA unless otherwise specified (Fig. 5-1 B, available at <https://doi.org/10.1523/JNEUROSCI.0777-18.2018>, f5-1). Resting potential was determined until stabilization of the membrane potential after the transition from voltage-clamp to current-clamp mode. 4-AP (Sigma-Aldrich) was diluted at the appropriate concentration in the external saline solution, and superfused to the recording chamber. Phrixotoxin-2 (PaTx2; Alomone Labs) was kept frozen for <2 months as 10 \times stock (10 μ M) aliquots and thawed immediately before experiments.

For cell-attached recordings, recording pipettes were filled with internal solution, with additional 200 mM BaCl₂ to prevent perforated patch effect mediated by high density of Kir channels in the pipettes. Cell attached configuration was achieved by gentle suction through a syringe. Recordings were performed in voltage-clamp mode without holding.

Action potential number was quantified using MiniAnalysis software for at least 1 min.

Experimental design and statistical analysis. The main objective of the present study was to investigate the sleep deficits in *DNK_v4* mutants of both sexes and the effects of Shal/K_v4 on neuronal excitability. Therefore, sleep measurements and electrophysiological recordings of GFP-labeled circadian neurons were performed on at least six flies for each genotype. The *n* number and gender of flies used in this study were described in the corresponding figure legends or results. For sleep measurements, as shown in Figures 1, 1-1 (available at <https://doi.org/10.1523/JNEUROSCI.0777-18.2018.f1-1>), 2, 2-1 (available at <https://doi.org/10.1523/JNEUROSCI.0777-18.2018.f2-1>), 3, 5-1A (available at <https://doi.org/10.1523/JNEUROSCI.0777-18.2018.f5-1>), 6A–C, 7, and 7-1 (available at <https://doi.org/10.1523/JNEUROSCI.0777-18.2018.f7-1>), each *n* corresponds to one animal. For electrophysiological recordings, as shown in Figures 4, 4-1 (available at <https://doi.org/10.1523/JNEUROSCI.0777-18.2018.f4-1>), 5, 5-1B (available at <https://doi.org/10.1523/JNEUROSCI.0777-18.2018.f5-1>), and 6D,E, each *n* corresponds to one cell, with one cell recorded per animal. We required an experimental result to be significantly different from both genetic controls (if applicable).

We used Student's *t* test for comparisons of two groups of normally distributed data using Sigma-AldrichPlot 10.0 software (RRID: SCR_003210), as shown in Fig.s 1-1D,G,J (available at <https://doi.org/10.1523/JNEUROSCI.0777-18.2018.f1-1>); 2J; 2-1A,B,E,F (available at <https://doi.org/10.1523/JNEUROSCI.0777-18.2018.f2-1>); 4E,J; 5A,C,F; 5-1A (available at <https://doi.org/10.1523/JNEUROSCI.0777-18.2018.f5-1>); and 7L,K,L. For multiple comparisons, one-way ANOVA followed by *post hoc* Tukey were performed using SPSS software (RRID:SCR_002865), as shown in Figures 1B,C,E,G,H,J; 1-1A (available at <https://doi.org/10.1523/JNEUROSCI.0777-18.2018.f1-1>); 2B–D,G,H,L; 2-1D,H (available at <https://doi.org/10.1523/JNEUROSCI.0777-18.2018.f2-1>); 3C; 4E; 4-1C,D (available at <https://doi.org/10.1523/JNEUROSCI.0777-18.2018.f4-1>); 5-1B (available at <https://doi.org/10.1523/JNEUROSCI.0777-18.2018.f5-1>); 6B,C,E,F; 7B,C,E,F; and 7-1B (available at <https://doi.org/10.1523/JNEUROSCI.0777-18.2018.f7-1>). For comparisons of non-normally distributed data (sleep bout duration), Mann–Whitney *U* tests were performed using SPSS software as shown in Figures 1D,I, 2E, and 7D. See Results and figure legends for specifics on statistical tests for each experiment. Statistical significance was set at $*p < 0.05$ and data are reported as mean \pm SEM.

Results

K_v4 is important for sleep in *Drosophila*

To determine whether K_v4 is important for regulating sleep in *Drosophila*, we first selected dominant-negative mutation, *UAS-DNK_v4*, and expressed it with the pan-neuronal driver (*elav/+*; *+;UAS-DNK_v4/+*, *DNK_v4*), which could completely eliminate K_v4 function (Ping and Tsunoda, 2011; Ping et al., 2015). Total and night-time sleep amounts were reduced in *DNK_v4* female flies (Fig. 1A,B; daytime: $F_{(2,120)} = 7.4$, $**p = 0.0046$, $p = 0.1056$; night-time: $F_{(2,120)} = 38.89$, *elav-GAL4* vs *elav>DNK_v4*, $**p < 0.0001$, *UAS-DNK_v4* vs *elav>DNK_v4*, $**p = 0.0009$; total: $F_{(2,120)} = 43.27$, $**p < 0.0001$; one-way ANOVA). Daytime sleep was not significantly reduced (Fig. 1A,B), and it might be due to a floor effect, because the control lines exhibited very little daytime sleep. The night-time sleep phenotypes were largely due to a decrease in sleep-bout duration (Fig. 1D; *elav-GAL4* vs *elav>DNK_v4*, $U = 164$, $p < 0.0001$; *UAS-DNK_v4* vs *elav>DNK_v4*, $U = 556.5$, $p = 0.001$. Mann–Whitney *U* test), because no significant change was found in sleep number and latency (Fig. 1C,E; sleep number: $F_{(2,120)} = 14.12$, $p = 0.1167$; latency: $F_{(2,120)} = 11.54$, $p = 0.6774$; one-way ANOVA). These results indicate that K_v4 can improve sleep maintenance and has sleep-promoting effects.

Next, we tested whether another null mutation of *Shal*⁴⁹⁵ could lead to sleep phenotypes observed in *DNK_v4* flies. Surprisingly, compared with background control (*w*¹¹¹⁸), night-time sleep was markedly increased in *Shal*⁴⁹⁵, without significant changes in daytime sleep (Fig. 1F,G; daytime: $F_{(2,160)} = 0.5637$, *w*¹¹¹⁸ vs *Shal*⁴⁹⁵, $p = 0.1732$, *Shal*⁴⁹⁵ vs *elav>K_v4;Shal*⁴⁹⁵, $p = 0.3318$; night-time: $F_{(2,160)} = 26.47$, *w*¹¹¹⁸ vs *Shal*⁴⁹⁵, $**p < 0.0001$, *Shal*⁴⁹⁵ vs *elav>K_v4;Shal*⁴⁹⁵, $p = 0.2351$; total: $F_{(2,160)} = 26.89$, *w*¹¹¹⁸ vs *Shal*⁴⁹⁵, $**p < 0.0001$, *Shal*⁴⁹⁵ vs *elav>K_v4;Shal*⁴⁹⁵, $p = 0.1879$; one-way ANOVA). Further analysis showed the increased sleep was due to lengthened sleep bout duration (Fig. 1H; sleep number: $F_{(2,160)} = 8.69$, *w*¹¹¹⁸ vs *Shal*⁴⁹⁵, $**p < 0.0001$; *Shal*⁴⁹⁵ vs *elav>K_v4;Shal*⁴⁹⁵, $p = 0.2004$, one-way ANOVA; *I*, sleep bout duration: *w*¹¹¹⁸ vs *Shal*⁴⁹⁵, $U = 432.8$, $**p = 0.0003$, *Shal*⁴⁹⁵ vs *elav>K_v4;Shal*⁴⁹⁵, $U = 641.3$, $p = 0.1374$, Mann–Whitney *U* test), suggesting that *Shal*⁴⁹⁵ mutation enhances sleep maintenance. Additionally, sleep latency in *Shal*⁴⁹⁵ mutant was increased significantly compared with control (Fig. 1J; $F_{(2,160)} = 11.45$, *w*¹¹¹⁸ vs *Shal*⁴⁹⁵, $**p = 0.0005$, *Shal*⁴⁹⁵ vs *elav>K_v4;Shal*⁴⁹⁵, $**p = 0.0034$; *w*¹¹¹⁸ vs *elav>K_v4;Shal*⁴⁹⁵, $p = 0.0894$, one-way ANOVA). Studies have shown that loss of *Shal/K_v4* could induce compensatory upregulation of *Shaker/K_v1* (Bergquist et al., 2010; Parrish et al., 2014). Moreover, *Shaker* mutants (*Sh*^{ms}) exhibited reduced sleep in *Drosophila*, even in heterozygous flies (Fig. 1-1B–D, available at <https://doi.org/10.1523/JNEUROSCI.0777-18.2018.f1-1>; sleep: $F_{(5,171)} = 32.56$, $**p < 0.0001$, $*p = 0.0035$ for night-time, $*p = 0.0054$ for total, one-way ANOVA; latency: $T_{(60)} = 3.25$, $*p = 0.0142$, *t* test). Thus, we assume that the increased sleep in *Shal*⁴⁹⁵ mutants could be caused by the upregulation of *Shaker*. Indeed, *Shal*⁴⁹⁵ mutant exhibited significant increase in *Shaker* expression as detected using qPCR (Fig. 1-1A, available at <https://doi.org/10.1523/JNEUROSCI.0777-18.2018.f1-1>; $F_{(2,14)} = 74.53$, $**p < 0.0001$, one-way ANOVA), whereas *Shaker* expression was not increased in *DNK_v4* mutants (Fig. 1-1A, available at <https://doi.org/10.1523/JNEUROSCI.0777-18.2018.f1-1>). Moreover, when *Shaker* function was inhibited in *shal*⁴⁹⁵ mutants, the animals exhibited reduced night-time sleep, similar as observed in *DNK_v4* expression animals (Fig. 1-1E–G, available at <https://doi.org/10.1523/JNEUROSCI.0777-18.2018.f1-1>; $F_{(5,147)} = 15.76$, $**p < 0.0001$, one-way ANOVA; $T_{(49)} = 3.87$, $p = 0.3155$, *t* test).

Subsequently, we tested whether the sleep phenotypes in *Shal*⁴⁹⁵ mutant could be rescued by overexpression of *Shal/K_v4* via the GAL4/UAS system. However, *Shal*⁴⁹⁵ mutant flies with *Shal* overexpression (*elav/+*; *UAS-K_v4/+*; *Shal*⁴⁹⁵) showed similar sleep time, as well as sleep number, sleep duration (Fig. 1F–I; statistics were shown above) and *Shaker* expression (Fig. 1-1A, available at <https://doi.org/10.1523/JNEUROSCI.0777-18.2018.f1-1>) compared with *Shal*⁴⁹⁵ mutants. Interestingly, there was a significant reduction in sleep latency after overexpressing K_v4 (Fig. 1J), indicating that the delayed sleep onset in *Shal*⁴⁹⁵ could be attributed to loss of K_v4, and not compensated by *Shaker* overexpression. Whereas *DNK_v4*-expressing flies did not show significant change in timing of sleep onset (Fig. 1E). We presume that the sleep phenotypes induced by pan-neuronal expression of *UAS-DNK_v4* may reflect an integrated effect of multiple regulatory mechanisms operating in different neuronal populations, as we will show later that *DNK_v4* expression in wake-promoting neurons delays sleep onset, but without effects on sleep onset when expressed in subsets of sleep-promoting neurons.

Loss of K_v4 function in l-LNvs delays sleep onset

We next tested sleep-regulating effects of K_v4 in subsets of circadian neurons. Studies have shown that l-LNvs, a group of wake-

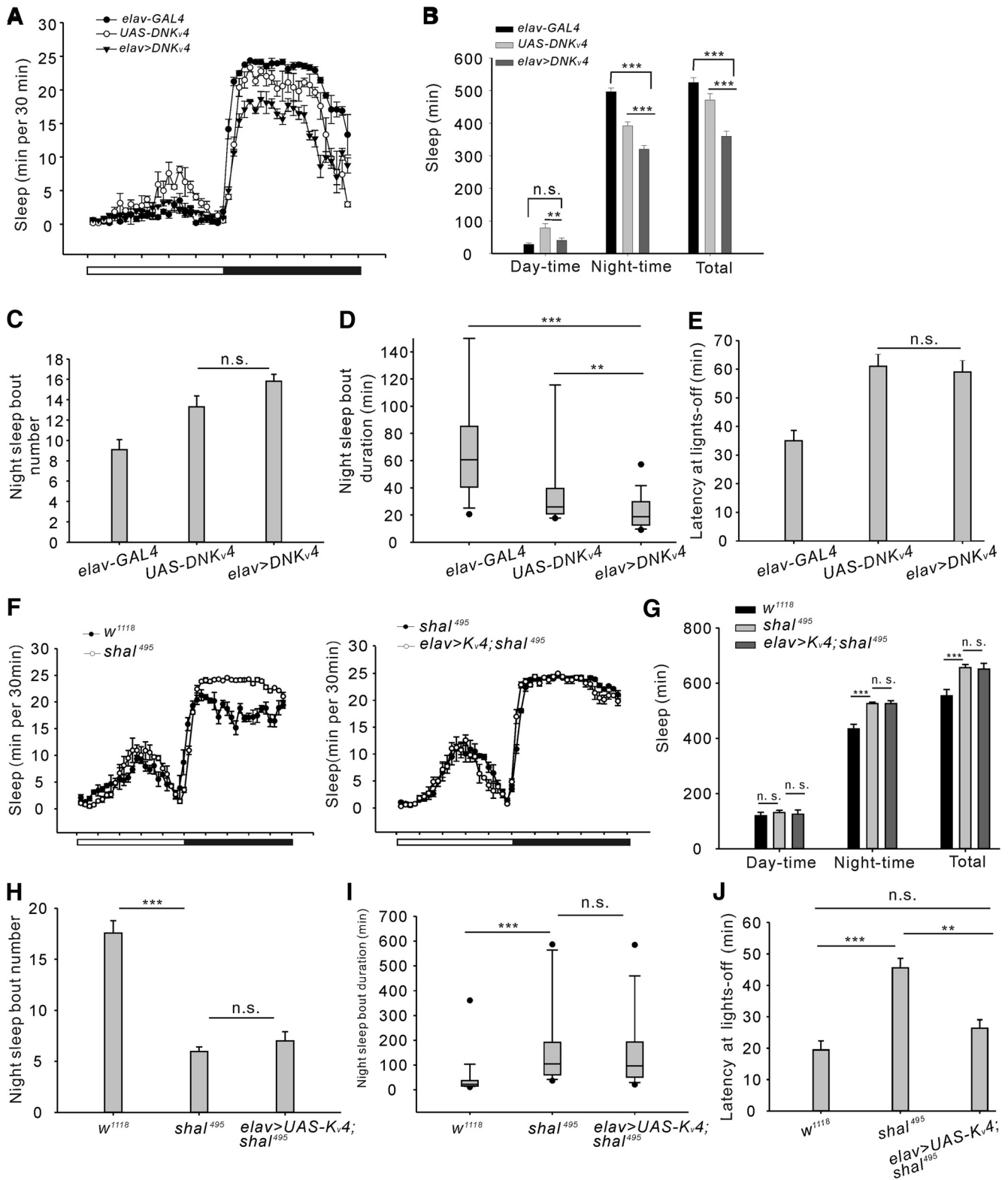


Figure 1. Sleep phenotypes in two different types of voltage-gated K^+ channel 4 (*Kv4*) mutants. **A**, Conventional sleep plots of controls (*elav-GAL4* and *UAS-DNKv4*, $n = 27$) and experimental flies (*elav > DNKv4*, $n = 69$) in 12 h LD. DN, dominant negative. White and black bars indicate 12 h light/dark periods, respectively. **B**, Total sleep amount (in 24 h) and sleep during daytime and nighttime in controls and experimental flies as described in **A**. **C**, Histograms of the number of night-time sleep bouts during night-time for controls and experimental flies. **D**, Box plots for night-time sleep bout duration. As the data are not normally distributed, box plots were used. The line inside the box indicates the median; the upper and lower box limits the 75 and 25% quantiles; vertical lines above and below the box represent the 90 and 10% quantiles; points show the 95% and 5% outliers. **E**, Sleep latency after lights-off at ZT12. Sleep latency was measured from the time lights-off to the onset of first sleep episode. **F**, Conventional sleep plots of *w¹¹¹⁸* ($n = 35$), *Shal⁴⁹⁵* ($n = 95$), and *Shal⁴⁹⁵* with *Kv4* overexpression lines (*elav > Kv4; Shal⁴⁹⁵*) ($n = 33$). **G–J**, Histograms of total sleep amount and sleep during daytime and night-time (**G**), night-time sleep bout number (**H**), night-time sleep bout duration (**I**), and sleep latency at lights-off (**J**). Mean \pm SEM is shown. * $p < 0.05$, ** $p < 0.01$, *** $p < 0.001$; n.s., not significant. Data are compared by Student's *t* test, except Mann–Whitney *U* test for comparison of nonparametrically distributed data. For multiple comparisons, one-way ANOVAs followed by *post hoc* Tukey were performed. For the quantification of *Shaker* mRNA expression levels in *Shal/Kv4* mutants and sleep deficits in *Shaker* mutants (Figure 1–1, available at <https://doi.org/10.1523/JNEUROSCI.0777-18.2018> f1–1).

promoting cells, regulate night-time sleep via GABA receptors (Agosto et al., 2008; Parisky et al., 2008; Liu et al., 2014). Thus, we first selected *pdf-GAL4* to drive expression of *UAS-DNK_v4* to eliminate K_v4 function (*pdf-GAL4/+;+;UAS-DNK_v4/+*) in small- (s-) and l-LNvs. Strikingly, sleep latency was markedly increased in *pdf>DNK_v4* female flies compared with controls, accompanied by decreased night-time sleep (Fig. 2A–C; latency: $F_{(2,108)} = 26.34$, $**p = 0.0076$, $*p = 0.0328$; sleep: $F_{(2,108)} = 8.31$, $p = 0.0631$, $**p = 0.0039$ for daytime, $F_{(2,108)} = 25.78$, $***p < 0.0001$ for night-time, $F_{(2,108)} = 9.62$, $p = 0.0733$, $***p = 0.0003$ for total, one-way ANOVA). Nevertheless, total and daytime sleep amounts did not exhibit a significant change (Fig. 2C). There was an increase in night sleep bout number, but night sleep bout duration was decreased (Fig. 2D; $F_{(2,108)} = 18.22$, *pdf-GAL4* vs *pdf>DNK_v4*, $*p = 0.0276$, *UAS-DNK_v4* vs *pdf>DNK_v4*, $*p = 0.0289$, one-way ANOVA, *E*, *pdf-GAL4* vs *pdf>DNK_v4*, $U = 223.5$, *UAS-DNK_v4* vs *pdf>DNK_v4*, $U = 336$, $***p < 0.0001$, Mann–Whitney *U* test). Delayed sleep onset latency was further confirmed using another *pdf-GAL4* on chromosome 2 (Fig. 2-1A, available at <https://doi.org/10.1523/JNEUROSCI.0777-18.2018.f2-1>; $T_{(72)} = 6.15$, $***p < 0.0001$, *t* test), and was also observed in male flies (Fig. 2-1B, available at <https://doi.org/10.1523/JNEUROSCI.0777-18.2018.f2-1>; $T_{(56)} = 5.46$, $*p = 0.0219$, *t* test). Moreover, increase or decrease in wakefulness was found in the early night by activating or inhibiting PDF cells, respectively (Fig. 1-1H–J, available at <https://doi.org/10.1523/JNEUROSCI.0777-18.2018.f1-1>; $F_{(5,174)} = 12.44$, $***p = 0.0003$ for daytime, $***p < 0.0001$ for night-time and total, one-way ANOVA; $T_{(57)} = 2.92$, $**p = 0.0051$, *t* test; Parisky et al., 2008). Restored K_v4 expression only in PDF cells partially rescued delayed sleep onset in *Shal⁴⁹⁵* flies (Fig. 2-1E, F, available at <https://doi.org/10.1523/JNEUROSCI.0777-18.2018.f2-1>; $T_{(53)} = 2.16$, $*p = 0.033$, *t* test). We did not observe significant change in circadian period in *pdf>DNK_v4* flies (Fig. 2-1C, available at <https://doi.org/10.1523/JNEUROSCI.0777-18.2018.f2-1>; *pdf-GAL4*: period = 23.7 ± 0.10 h; *UAS-DNK_v4*: period = 23.8 ± 0.12 h; *pdf>DNK_v4*: 24.1 ± 0.11 h; $F_{(2,93)} = 11.03$, *pdf-GAL4* vs *pdf>DNK_v4*, $p = 0.0842$, *UAS-DNK_v4* vs *pdf>DNK_v4*, $p = 0.1037$, one-way ANOVA). Downregulation of K_v4 expression in PDF cells (*pdf>Shal-RNAi*) also delayed sleep onset (Fig. 2-1G, H, available at <https://doi.org/10.1523/JNEUROSCI.0777-18.2018.f2-1>; $F_{(2,76)} = 51.76$, *UAS-Shal-RNAi* vs *pdf>Shal-RNAi*, $**p = 0.0039$, *pdf-GAL4* vs *pdf>Shal-RNAi*, $**p = 0.0054$, one-way ANOVA), consistent with the results of *DNK_v4*.

To examine the specific roles of s- and l-LNvs, we overexpressed *DNK_v4* with the *c929-GAL4* driver, which drives expression in l-LNvs, but not s-LNvs. We found that sleep latency was increased in *c929>DNK_v4* flies, accompanied by decreased daytime and night-time sleep amounts. Since *pdf-GAL80* would suppress the transcription activity of *GAL4* in s/l-LNvs, we assayed the sleep phenotype of *c929>DNK_v4* flies expressing *pdf-GAL80* (*c929-GAL4/+;UAS-DNK_v4/+;pdf-GAL80/+*). These flies exhibited decreased sleep latency and increased night-time sleep, compared with *c929>DNK_v4* flies (Fig. 2F, G; $F_{(2,89)} = 91.29$, $**p = 0.0063$; *H*, daytime: $F_{(2,89)} = 2.31$, $p = 0.2318$, night-time: $F_{(2,89)} = 65.49$, $***p < 0.0001$; total: $F_{(2,89)} = 78.39$, $***p < 0.0001$, one-way ANOVA). These results further support that K_v4 functions to control sleep onset in l-LNvs, but not s-LNvs.

To rule out the possibility that the increased sleep latency was caused by an enhanced startle response to lights-off, we examined sleep in *pdf>DNK_v4* flies under constant darkness (Day 1 of DD), and assayed the time it took flies to fall asleep from CT12. The increase of sleep latency persisted in DD (Fig. 2I; latency at CT12,

51 ± 10.4 min for *UAS-DNK_v4*, 163 ± 19.7 min for *pdf>DNK_v4*, $T_{(59)} = 5.23$, $***p < 0.0001$, *t* test). Next, to bypass possible complications from the persistent K_v4 expression during development, we induced *pdf-GAL4* along with *tub-GAL80^{ts}*, which inhibits *GAL4* function in a temperature-dependent manner, to silence K_v4 expression during development and switch the expression on in the adulthood. Compared with control lines, sleep latency of *pdf>DNK_v4;tub-GAL80^{ts}* was significantly increased (Fig. 2J, K; $F_{(2,73)} = 107.5$, *pdf-GAL4* vs *pdf>DNK_v4;tub-GAL80^{ts}*, $**p = 0.0021$, *tub-GAL80^{ts}*; *UAS-DNK_v4* vs *pdf>DNK_v4;tub-GAL80^{ts}*, $**p = 0.0028$, one-way ANOVA).

No significant change in sleep onset was observed by blocking K_v4 activity in DN1s

Wake–sleep transition is expected to be determined by integration of signals from both wake- and sleep-promoting neurons. Next we examined whether K_v4 in sleep-promoting neurons also regulates sleep onset. Because reports show activation of DN1s promotes sleep at dusk (Kunst et al., 2014; Guo et al., 2016), we first selected *clk4.1M-GAL4* to drive expression of *UAS-DNK_v4* to eliminate K_v4 function in DN1s. Sleep latency at lights-off was not changed by inhibiting K_v4 function in DN1s (Fig. 3A, C; $F_{(2,84)} = 47.78$, $p = 0.1068$, one-way ANOVA). We then used another DN1s driver, *R18H11-GAL4*, and further confirmed no significant change in sleep latency by inhibiting K_v4 function compared with controls (Fig. 3B, C; $F_{(2,84)} = 24.37$, $p = 0.0927$, one-way ANOVA). Moreover, we did not observe any significant change in circadian period in *R18H11>DNK_v4* flies compared with controls (Fig. 2-1D, available at <https://doi.org/10.1523/JNEUROSCI.0777-18.2018.f2-1>).

K_v4 channels regulate excitability of circadian neurons

Next, we investigated how *DNK_v4* regulates sleep onset. We first tested whether *DNK_v4* expression eliminates *I_A* in the circadian neurons. We chose *pdf-GAL4*, *clk4.1M-GAL4* and *50y-GAL4* to drive *DNK_v4* and GFP expression in l-LNvs (*UAS-CD8GFP; pdf-GAL4/+;UAS-DNK_v4/+*), DN1s (*UAS-CD8GFP; clk4.1M-GAL4/+;UAS-DNK_v4/+*), and PI (*UAS-CD8GFP; 50y-GAL4/+;UAS-DNK_v4/+*) neurons, respectively. *I_A* was almost completely inhibited by expressing *DNK_v4* in l-LNvs and PI cells (Fig. 4A, B, E; l-LNvs: $T_{(12)} = 54.33$; PI cells: $T_{(12)} = 54.33$, $***p < 0.0001$, *t* test, *F*). However, we still detected remaining *I_A* component in DN1s, and all the *I_A* components were completely blocked by a specific *I_A* inhibitor, 4-AP (Fig. 4C, E; $F_{(2,19)} = 33.42$, $*p = 0.0239$, $***p < 0.0001$, one-way ANOVA), indicating that Shaker/K_v1 mediates the majority of *I_A* in DN1s, compared with K_v4. Subsequently, specific interference of K_v4 function did not significantly change the excitability of DN1s (Fig. 4-1, available at <https://doi.org/10.1523/JNEUROSCI.0777-18.2018.f4-1>). A remaining *I_A* component was also detected in l-LNvs in *Shal⁴⁹⁵* mutants (*UAS-CD8GFP; pdf-GAL4/+;Shal⁴⁹⁵*) (Fig. 4D, E; $F_{(2,20)} = 55.72$, $***p < 0.0001$, one-way ANOVA). As previously stated in motor neurons, remaining *I_A* currents could be contributed by overexpression of *Shaker* (Bergquist et al., 2010).

To confirm *I_A* regulates membrane excitability of circadian neurons, we monitored spontaneous neuronal activity in the presence of 4-AP. We used cell-attached voltage-clamp of neuronal activity without changing the cytoplasmic milieu to record action potential (AP) currents. As reported previously (Cao and Nitabach, 2008; Sheeba et al., 2008b; Depetris-Chauvin et al., 2011), l-LNvs exhibited tonic and burst AP currents at ZT9 (Fig. 4G). 4-AP significantly increased frequency of AP currents, which were completely blocked by TTX in l-LNvs (Fig. 4G, J; $T_{(13)} = 4.96$,

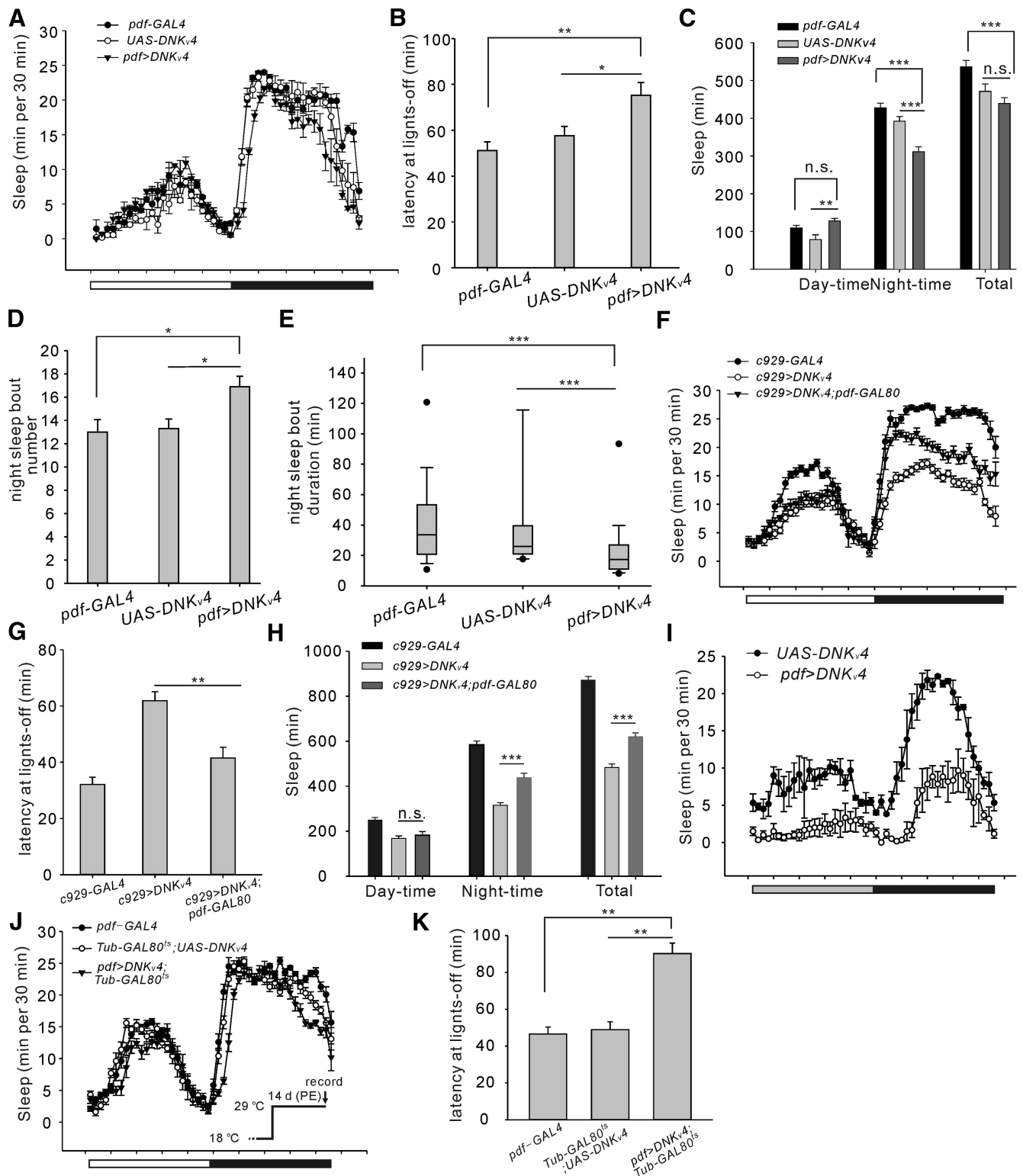


Figure 2. *K_v4* in pigment-dispersing factor (PDF) cells regulates sleep onset. **A**, Conventional sleep plots of controls (*pdf-GAL4* and *UAS-DNK_v4*, $n = 32$) and experimental flies (*pdf>DNK_v4*, $n = 47$) in LD. **B–E**, Quantification of sleep latency after lights-off (**B**), and other sleep parameters showing total sleep amount and sleep during daytime and night-time (**C**), night-time sleep bout number (**D**) and night-time sleep duration (**E**). **F**, Conventional sleep plots of the transgenic lines, including *c929-GAL4* ($n = 31$), *c929>DNK_v4* ($n = 33$), and *c929>DNK_v4;pdf-GAL80* ($n = 28$). **G**, **H**, Quantification of sleep latency and sleep amount of flies shown in **F**. **I**, Conventional sleep plots in DD of control (*UAS-DNK_v4*, $n = 30$) and experimental (*pdf>DNK_v4*, $n = 31$) flies. Gray and black bars indicate 12 h subjective day and night, respectively. Note that sleep latency at subjective night was increased by expressing *DNK_v4* in DD. **J**, **K**, Conventional sleep plots of controls (*pdf-GAL4* and *Tub-GAL80^{ts};UAS-DNK_v4*, $n = 22$, and 27, respectively) and experimental flies (*pdf>DNK_v4;Tub-GAL80^{ts}*, $n = 27$) at 29°C in LD (**J**) and quantification of sleep latency (**K**; inset procedure). Mean \pm SEM is shown. * $p < 0.05$, ** $p < 0.01$, *** $p < 0.001$, n.s., not significant. Data are compared by Student's *t* test, except Mann–Whitney *U* test for comparison of nonparametrically distributed data. For multiple comparisons, one-way ANOVAs followed by *post hoc* Tukey were performed. For the quantification of sleep onset in males, *Shal-RNAi* mutants and circadian period (Figure 2-1, available at <https://doi.org/10.1523/JNEUROSCI.0777-18.2018.f2-1>).

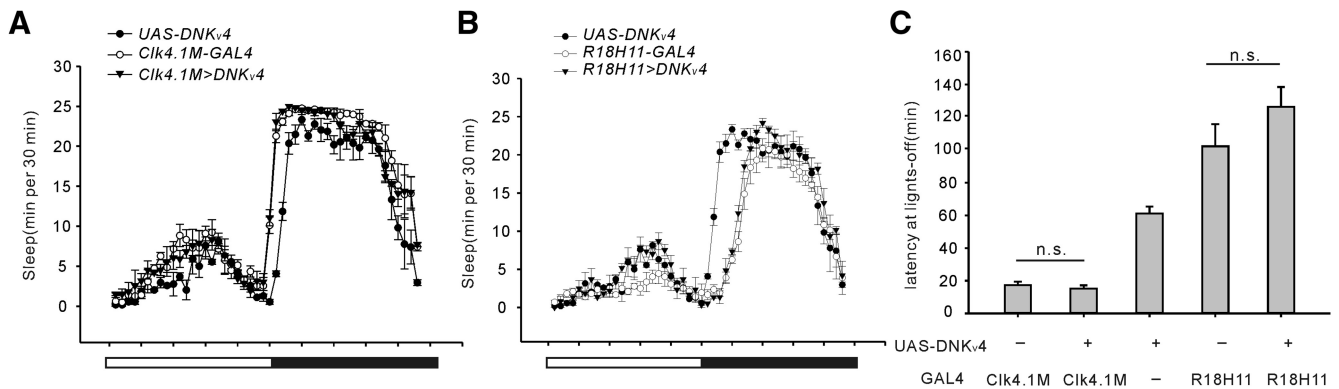


Figure 3. Interference of K_v4 in dorsal neurons (DN1s) does not significantly regulate sleep onset. **A, B**, Conventional sleep plots of controls (*Ck4.1M-GAL4*, *UAS-DNK_{v4}*, and *R18H11-GAL4*; $n = 27$ – 32) and experimental flies (*Ck4.1M>DNK_{v4}* and *R18H11>DNK_{v4}*; $n = 30$) in LD cycles. **C**, Quantification of sleep latency after lights-off. Mean \pm SEM is shown. n.s., not significant. One-way ANOVAs followed by *post hoc* Tukey were performed. Data are compared by one-way ANOVAs followed by *post hoc* Tukey.

$*p = 0.0143$, *t* test). Similarly, 4-AP also increased neuronal AP currents in GFP-labeled PI and DN1s (Fig. 4*H–J*; $T_{(13)} = 3.66$, $**p = 0.0029$, $T_{(21)} = 2.80$, $*p = 0.0107$, *t* test).

DNK_{v4} induces neuronal hyperactivity in a time-of-day-dependent manner

Since K_v4 in l-LNVs specifically controls sleep onset at dusk, we next asked whether I_A varies throughout the day in l-LNVs. However, our results showed that there was no difference in I_A amplitudes between ZT1 (dawn) and ZT13 (dusk; Fig. 5*A*; 318 ± 17.3 pA at ZT1, 309 ± 15.1 pA at ZT13, $T_{(22)} = 0.75$, $p = 0.5549$, *t* test). We also compared steady-state inactivation properties of K_v4 currents in neurons. No difference was observed between ZT1 and ZT13 in half-maximal inactivation potential values (Fig. 5*B*; $T_{(20)} = 1.36$, $p = 0.1873$, *t* test).

The membrane excitability and Ca²⁺ waves of l-LNVs and PI neurons was reported to be strongly rhythmic (Cao and Nitabach, 2008; Sheeba et al., 2008b; Barber et al., 2016; Liang et al., 2016). Our cell-attached recordings of GFP-labeled l-LNVs (*pdf > CD8GFP*) revealed a pattern of circadian regulation of spontaneous AP currents, with higher firing rate during daytime than night-time (Fig. 5*D, F*; $F_{(5,41)} = 141.40$, $***p < 0.0001$, one-way ANOVA). We detected different kinds of firing properties of l-LNVs, including no firing cells, tonic firing cells, bursting cells, and cells mixed with tonic firing and bursting (Fig. 5*E*). Blocking K_v4 function in l-LNVs by *DNK_{v4}* expression (*pdf > CD8GFP; DNK_{v4}*) increased the frequency of AP currents during dusk (~ZT13; Fig. 5*D, F*; ZT9: $T_{(14)} = 2.55$, $*p = 0.0230$; ZT13: $T_{(13)} = 4.07$, $**p = 0.0053$; ZT17: $T_{(14)} = 2.50$, $*p = 0.0306$, *t* test), but without effects on firing frequency during dawn (~ZT1). It appears that loss of K_v4 function did not upregulate the firing rate when activity was relatively high (ZT1, 5, 17, and 21). Moreover, we found that the resting membrane potential (RMP) of l-LNVs exhibited circadian oscillations, with more depolarized RMPs at dawn, declining to lower levels at dusk (from -45 mV at ZT1 to -54 mV at ZT13; Fig. 5*C*; -45.6 ± 2.0 mV at ZT1, -54.2 ± 1.8 mV at ZT13, $T_{(11)} = 2.83$, $*p = 0.0162$, *t* test). K_v4-mediated I_A was sensitive to the pre-pulse window between -60 mV and -40 mV (Fig. 5*B*), indicating that more K_v4 channels were inactivated at ZT1 when RMPs were relatively depolarized. To confirm membrane potential oscillation contributes to time-of-day-dependent regulation of excitability by K_v4, l-LNVs were artificially hyperpolarized from ~ -45 to ~ -55 mV at ZT1 by current injection during recordings in Figure 5*C*. Firing frequency was not significantly increased at RMPs by Patx2 (K_v4-specific blocker)

perfusion at ZT1, but it was significantly increased when the membrane potential was hyperpolarized to -55 mV by current injection (Fig. 5-1*B*, available at <https://doi.org/10.1523/JNEUROSCI.0777-18.2018.f5-1>; $F_{(3,27)} = 199.5$, $p = 0.1657$, $**p = 0.0026$, one-way ANOVA). Because I_A was mainly contributed by Shaker/K_v1 in DN1s, DNK_{v4} expression in DN1s did not change the frequency and oscillation of AP currents (*Ck4.1M>CD8GFP;DNK_{v4}*) (Fig. 4-1, available at <https://doi.org/10.1523/JNEUROSCI.0777-18.2018.f4-1>). Thus, although K_v4 maintains its expression during the day and night, it may still preferentially control excitability of neurons at dusk due to oscillation of RMPs in wake-promoting neurons.

To demonstrate that the activity of PDF neurons at dusk is crucial for sleep onset, we selectively activated PDF neurons at dusk (ZT9–12 and ZT12–15) by dTrpA1 expression. Our results show that activating PDF neurons during ZT12–15 significantly delayed sleep onset, compared with activation during ZT9–12 (Fig. 5-1*A*, available at <https://doi.org/10.1523/JNEUROSCI.0777-18.2018.f5-1>; $T_{(38)} = 8.84$, $***p < 0.0001$, $T_{(38)} = 1.95$, $p = 0.1076$, *t* test). These results indicate that control of the firing of l-LNVs at dusk by K_v4 is essential for normal sleep onset.

PDF is necessary for delayed sleep onset in DNK_{v4} mutants

To determine whether neuropeptide PDF is required for the delayed sleep onset in *pdf > DNK_{v4}* flies, we examined sleep behavior in *pdf⁰¹* flies that lack PDF. Compared with PDF-null background controls, *pdf > DNK_{v4}; pdf⁰¹* flies showed decreased total sleep time, but no difference was found in sleep latency (Fig. 6*A–C*; daytime: $F_{(2,84)} = 0.34$, $p > 0.05$; night-time: $F_{(2,84)} = 23.65$, $**p = 0.0034$, $***p = 0.0008$; total: $F_{(2,84)} = 23.96$, $***p < 0.0001$, one-way ANOVA). Furthermore, we determined whether DNK_{v4} would still induce circadian-dependent hyperactivity in l-LNVs in PDF-null background. Excitability and RMPs of l-LNVs still exhibited circadian oscillation in the absence of PDF (Fig. 6*D–F*; $F_{(3,27)} = 203.5$, $*p = 0.0260$, one-way ANOVA). More importantly, compared with PDF-null background control, loss of K_v4 function still preferentially increased frequency of AP currents at dusk (ZT13), suggesting that lack of PDF has little effect on the regulation of neuronal excitability by K_v4. In summary, l-LNVs hyperactivity induced by DNK_{v4} expression delayed sleep onset in a PDF-dependent mechanism.

K_v4 also regulates timing of sleep onset in circadian output area

We set out to identify possible downstream neurons involved in K_v4-mediated sleep onset delay. PI is developmentally and functionally analogous to the hypothalamus in vertebrates (Foltényi

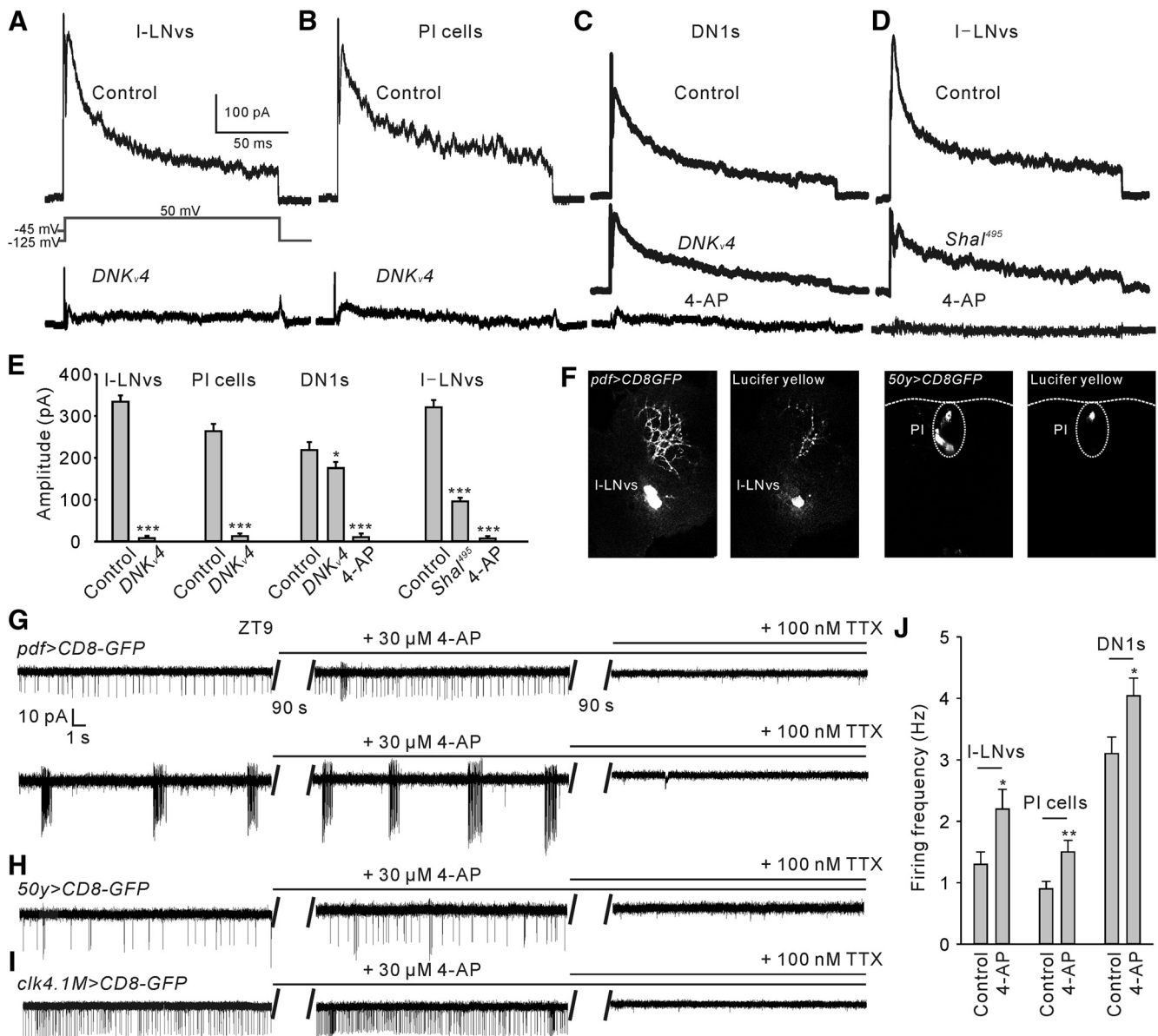


Figure 4. K_v4 contributes to A-type currents (I_A) and regulates activities in subsets of circadian neurons. **A**, Shown are representative voltage-clamp recordings of I_A from I-LNvs in two genotypes: *pdf>CD8GFP* (Control) and *pdf>CD8GFP;DNK_{v4}* (*DNK_{v4}*). We first recorded total whole-cell K^+ current, which was elicited by a 500 ms prepulse of -125 mV with a voltage jump to $+50$ mV. Then K_v4 (or I_A) is completely inactivated and the total delayed rectifier (DR) current remains with a prepulse of $+45$ mV. I_A trace obtained by subtracting the DR current trace from the total K^+ current trace. **B**, Shown are representative recordings of I_A from PI neurons in two genotypes: *50y>CD8GFP* and *50y>CD8GFP;DNK_{v4}*. **C**, Shown are representative recordings of I_A from DN1s in two genotypes: *clk4.1M>CD8GFP* and *clk4.1M>CD8GFP;DNK_{v4}*, in the presence or absence of 2 mM 4-AP. **D**, Shown are representative recordings of I_A from large ventral lateral neurons (I-LNvs) in two genotypes: *pdf>CD8GFP* and *pdf>CD8GFP;Sha1⁴⁹⁵*, in the presence or absence of 4-AP. **E**, Quantification of I_A amplitudes recorded from the genotypes shown in **A–D**. Note that there is still remaining I_A (~ 100 pA) in *clk4.1M>CD8GFP;DNK_{v4}* (DN1s) and *Sha1⁴⁹⁵* (I-LNvs) mutants; $n = 6–9$ for each case. **F**, GFP-labeled PDF cells and a typical Lucifer yellow-filled I-LNv during recording (left two). GFP-labeled pars intercerebralis (PI) cells and a typical Lucifer yellow-filled PI neuron during recording (right two). **G**, Two typical firing patterns (tonic and burst firing) as shown in the up and down panels in GFP-labeled I-LNvs. 4-AP, a specific I_A blocker, increased firing rate in both firing patterns at ZT9, and all the AP currents could be completely inhibited by TTX. **H**, **I**, 4-AP also increased firing rate in PI neurons and DN1s, and all the AP currents were blocked by TTX. **J**, Quantification of firing frequency in the cells as shown in **G–I**; $n = 6–12$ for each case. Mean \pm SEM is shown. * $p < 0.05$, ** $p < 0.01$, *** $p < 0.001$. Data are compared by Student's *t* test. For multiple comparisons, one-way ANOVAs followed by *post hoc* Tukey were performed. For the comparison of RMPs and firing rate in DN1s between control and *DNK_{v4}* mutants (Figure 4-1, available at <https://doi.org/10.1523/JNEUROSCI.0777-18.2018.f4-1>).

et al., 2007; de Velasco et al., 2007), and has been established as an important component of the circadian output pathway for rest: activity rhythms under circadian control (Cavanaugh et al., 2014; Cavey et al., 2016). We next chose *50y-GAL* to drive the expression of *DNK_{v4}* in subsets of PI neurons (*w;50y-GAL4/+;UAS-DNK_{v4}/+*), which has been shown to regulate sleep (Foltenyi et al., 2007). Interestingly, compared with controls (*w;+;UAS-DNK_{v4}/+*, and *w;50y-GAL4/+;+*), *50y-GAL4>UAS-DNK_{v4}* showed difficulty in falling asleep after lights-off as well, ac-

companied with significantly reduced night-time sleep amount and bout number (Fig. 7A,B; daytime: $F_{(2,105)} = 2.357$, *UAS-DNK_{v4}* vs *50y-GAL4>DNK_{v4}*, $p = 0.0807$, *50y-GAL4* vs *50y-GAL4>DNK_{v4}*, $p = 0.1094$, night-time: $F_{(2,105)} = 123.0$, *** $p < 0.0001$; total: $F_{(2,105)} = 89.77$, *UAS-DNK_{v4}* vs *50y-GAL4>DNK_{v4}*, *** $p < 0.0001$, *50y-GAL4* vs *50y-GAL4>DNK_{v4}*, ** $p = 0.0034$, one-way ANOVA; C, $F_{(2,105)} = 44.97$, *UAS-DNK_{v4}* vs *50y-GAL4>DNK_{v4}*, *** $p < 0.0001$, *50y-GAL4* vs *50y-GAL4>DNK_{v4}*, *** $p = 0.0008$, one-way ANOVA; D, *UAS-*

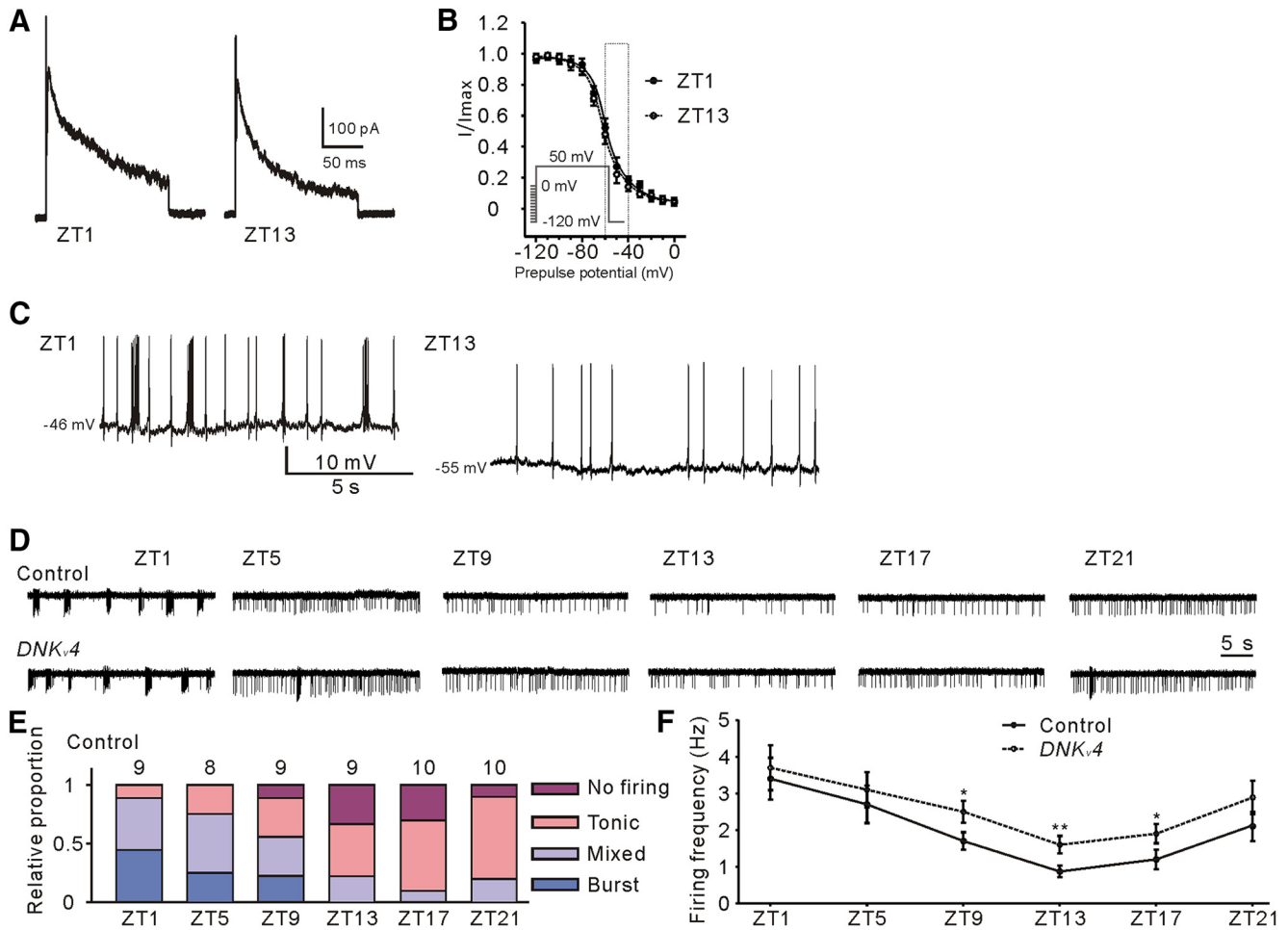


Figure 5. K_v4 controls membrane excitability at dusk. **A**, Shown are representative recordings of *I_A* from GFP-labeled I-LNvs at ZT1 and ZT13. Note that there is no significant change in *I_A* amplitudes. *n* = 12 for ZT1 and *n* = 13 for ZT13. **B**, Steady-state inactivation properties of K_v4 at ZT1 and ZT13. We used a pre-pulse from −120 to 0 mV, in 10 mV intervals, then stepped to a test potential of +50 mV (inset, procedure). Steady-state inactivation curves were fitted with Boltzmann function: $I/I_{max} = 1/(1 + \exp[(V - V_{1/2})/k])$. There was no significant difference in half-maximal inactivation potential values (*V*_{1/2}). (ZT1: *V*_{1/2} = −59.3 ± 1.9 mV, *n* = 11; ZT13: *V*_{1/2} = −61.5 ± 3.1 mV, *n* = 11). **C**, Representative spontaneous firing traces (at ZT1 and ZT13) showing resting membrane potential (RMP) values of GFP-labeled I-LNvs by current-clamp recordings. Note that RMP is significantly depolarized at ZT1 compared with ZT13; *n* = 6 for ZT1 and *n* = 7 for ZT13. **D**, Representative spontaneous firing patterns (cell-attached) are shown at the indicated time of recordings in control (*pdf*>*CD8GFP*) or *DNK_v4*-expressing I-LNvs (*pdf*>*DNK_v4;CD8GFP*). Note that I-LNvs exhibit circadian oscillation of firing, with higher firing frequency at dawn and lower firing frequency at dusk. **E**, Relative proportions of firing phenotypes from I-LNvs at the indicated time of the circadian day. **F**, Quantification of firing rates at the indicated time of the circadian day as shown in **E**. Loss of K_v4 resulted in increased firing rate preferentially at dusk, when the firing frequency and RMP are relatively lower in I-LNvs; *n* = 8–10 for each case. Mean ± SEM is shown. **p* < 0.05, ***p* < 0.01. Data are compared by Student's *t* test. For multiple comparisons, one-way ANOVAs followed by *post hoc* Tukey were performed. For the comparison of sleep onset by activating PDF cells between ZT9–12 and ZT12–15 (Figure 5-1A, available at <https://doi.org/10.1523/JNEUROSCI.0777-18.2018.f5-1>). For the comparison of firing rate between control and PaTx2-treated I-LNvs at different membrane potentials, (Figure 5-1B, available at <https://doi.org/10.1523/JNEUROSCI.0777-18.2018.f5-1>).

DNK_v4 vs *50y-GAL4*>*DNK_v4*, *U* = 619, *p* = 0.2139, *50y-GAL4* vs *50y-GAL4*>*DNK_v4*, *U* = 716.5, *p* = 0.1082, Mann–Whitney *U* test; *F*, *F*_(2,105) = 10.54, ****p* = 0.0002, ***p* = 0.0038, one-way ANOVA). These flies exhibited very little daytime sleep in LD (Fig. 7A, B) and lengthened sleep latency in DD (Fig. 7H, I; *T*₍₅₄₎ = 11.88, ****p* < 0.0001, *t* test). Most (>80%) of the mutants became arrhythmic under DD and the rhythmic ones had a ~25.4 h period phenotype (Fig. 2-1D, available at <https://doi.org/10.1523/JNEUROSCI.0777-18.2018.f2-1>; *F*_(2,59) = 5.92, **p* = 0.0106, ****p* = 0.0004, one-way ANOVA). To exclude the possibility that the reduction of sleep amount is due to animals' hyperactivity, we calculated waking activity (activity counts per minute awake) and no hyperactivity was found, but with a mild hypoactivity (Fig. 7E; *F*_(2,105) = 7.29, **p* = 0.0268, ****p* = 0.0007, one-way ANOVA). We also observed delayed sleep onset in male flies (Fig. 7-1, available at <https://doi.org/10.1523/JNEUROSCI.0777-18.2018.f7-1>; *F*_(2, 79) = 49.9, ***p* = 0.0026, ****p* <

0.0001, one-way ANOVA). All these results suggest that K_v4 in PI neurons is also required to control sleep onset, but without effects on the sleep maintenance.

We next asked whether the defective sleep initiation was due to the hyperactivity of PI neurons. Expression of the temperature-gated nonspecific cation channel dTrpA1 driven by *50y-GAL4* can impose a fast firing pattern on the cell at 29°C. Similar to *50y*>*DNK_v4* mutants, *50y*>*dTrpA1* flies also exhibited markedly longer sleep latency (Fig. 7F, G; *T*₍₆₇₎ = 4.27, ****p* < 0.0001, *t* test). This result verified the notion that function loss of K_v4 could lead to hyperactivity of neurons and subsequent delayed sleep onset.

We examined whether PDF receptors in PI neurons regulate sleep onset. Interestingly, downregulation of PDFR by expressing *pdfR-RNAi* in PI cells (*50y*>*pdfR-RNAi*) significantly advanced sleep onset, accompanied with increased night-time sleep amount (Fig. 7J, K; daytime: *T*₍₅₂₎ = 0.18, *p* = 0.2541, night-time: *T*₍₅₂₎ =

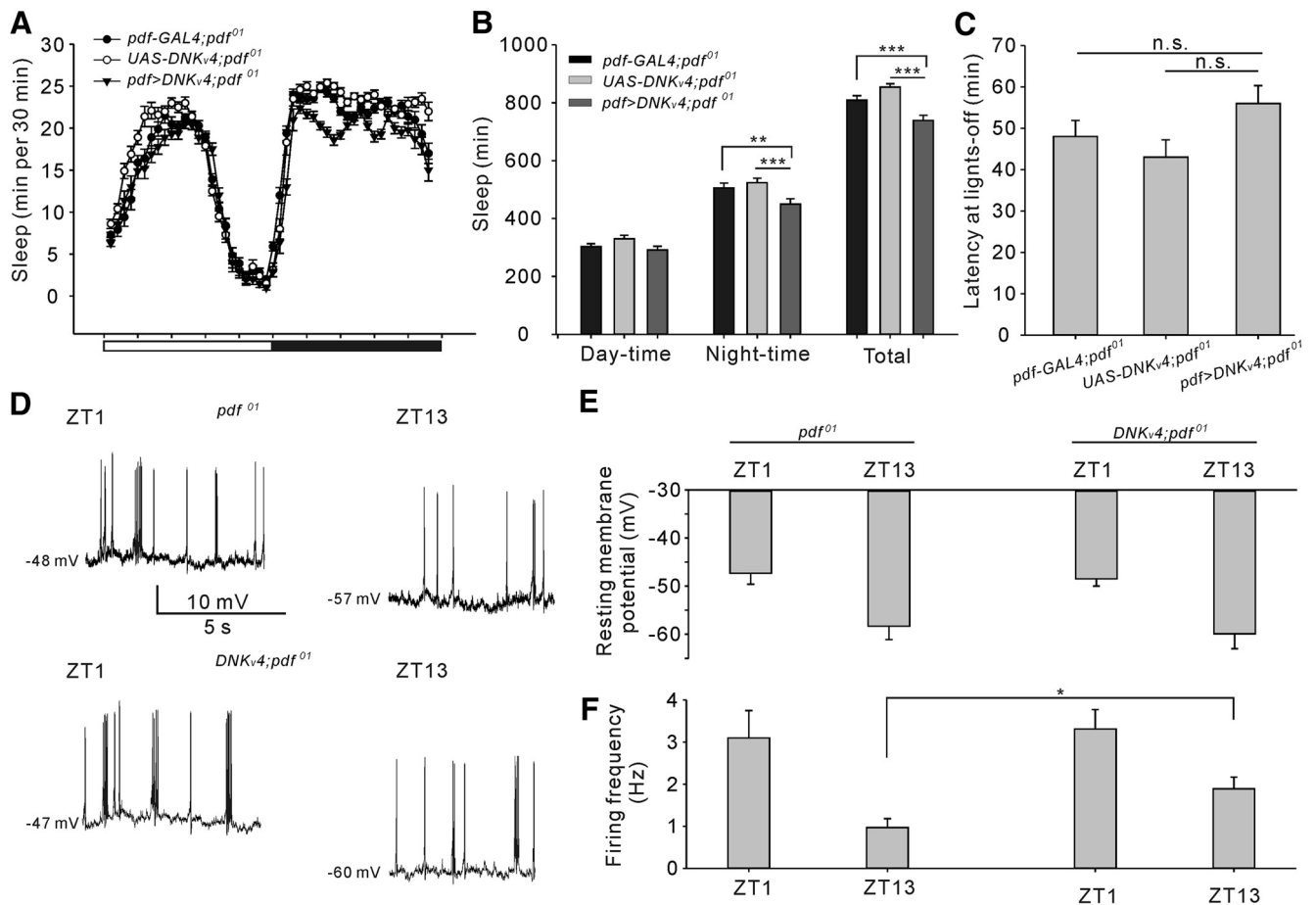


Figure 6. PDF is required for *DNKv4*-mediated delayed sleep onset in PDF neurons. **A**, Conventional sleep plots of indicated transgenic lines, including *pdf-GAL4;pdf⁰¹* ($n = 33$), *UAS-DNKv4;pdf⁰¹* ($n = 27$), and *pdf>DNKv4;pdf⁰¹* ($n = 27$). **B, C**, Quantification of sleep amount (**B**) and sleep latency (**C**) of flies shown in **A**. **D**, Representative spontaneous firing traces showing RMP values of GFP-labeled I-LNvs in *pdf⁰¹* background flies by current-clamp recordings. Recordings were performed at ZT1 and ZT13 and two transgenic lines were used (*pdf>CD8GFP;pdf⁰¹* and *pdf>CD8GFP;DNKv4;pdf⁰¹*). **E, F**, Quantification of RMPs and firing frequency of I-LNvs recorded in **D**. Mean \pm SEM is shown. $*p < 0.05$, $**p < 0.01$, $***p < 0.001$; n.s., not significant. One-way ANOVAs followed by *post hoc* Tukey were performed.

5.85, $***p < 0.0001$, $T_{(52)} = 5.89$, $***p < 0.0001$, t test; L , $T_{(52)} = 3.19$, $*p = 0.0114$, t test). These results suggest that PDF neurons may act on downstream PI neurons to regulate night-time sleep, and *K_v4* in these neurons regulates sleep onset likely through regulating PDF/PDFR signaling.

Discussion

To the best of our knowledge, this is the first demonstration of the function of *K_v4* in sleep regulation. In this study, we showed that *K_v4* is important for night-time sleep in *Drosophila*, and is especially crucial to normal sleep onset. Pan-neuronal expression of *DNKv4* leads to decreased night-time sleep, indicating a general sleep-promoting function of *K_v4*. The increased night-time sleep in *Shal⁴⁹⁵-null* mutant reveals a compensatory overexpression of *Shaker*. A transcription factor named *Kruppel* (*Kr*) was identified to be a central regulator of this process (Parrish et al., 2014), consistent with our conclusion that the compensatory modulation occurs at the transcriptional level. However, the *Kr* expression is suggested to be a result from detecting *K_v4* or *Shaker/K_v1* conductance, since 4-AP also increased *Shaker* RNA expression (Parrish et al., 2014). In our study, we did not observe significant increase in *Shaker* RNA expression in *DNKv4* mutants suggesting that other transcription factor(s), rather than *Kr*, may be involved in regulating *Shal/K_v4* and *Shaker* balance.

Previous studies have shown that cyclin A and GABA_A receptors (or RDL) in circadian neurons also regulate sleep latency (Agosto et al., 2008; Rogulja and Young, 2012; Afonso et al., 2015). A molecule named WAKE interacts with RDL, and the cycling manner of WAKE promotes excitability oscillation of I-LNvs (Liu et al., 2014). Moreover, DN1s may regulate wake-sleep transition at dusk in a clock-dependent manner (Kunst et al., 2014; Guo et al., 2016). Our results verified that *K_v4*-mediated I_A in I-LNvs, and function-loss of *K_v4* preferentially upregulated membrane excitability at dusk, although *K_v4* expression was not rhythmic. Moreover, RMP values exhibit circadian oscillation in I-LNvs, with depolarized RMPs at dawn. Thus, less *K_v4* channels would be available for opening when RMPs are depolarized. This supports our data showing that blocking *K_v4* did not significantly increase firing rate when circadian neurons were hyperexcitable at dawn. Although RMPs and firing rate also exhibit circadian oscillation in DN1s (Fig. 4-1, available at <https://doi.org/10.1523/JNEUROSCI.0777-18.2018.f4-1>), blocking *K_v4* activity has no effects on sleep latency. We further demonstrated that this may be caused by the near absence of *K_v4*-mediated I_A in DN1s. Thus, *K_v4* controls wake-sleep transition at dusk in subsets wake-promoting cells, but not in DN1s. The phases of Ca^{2+} waves recorded with a fine temporal resolution were approximately co-

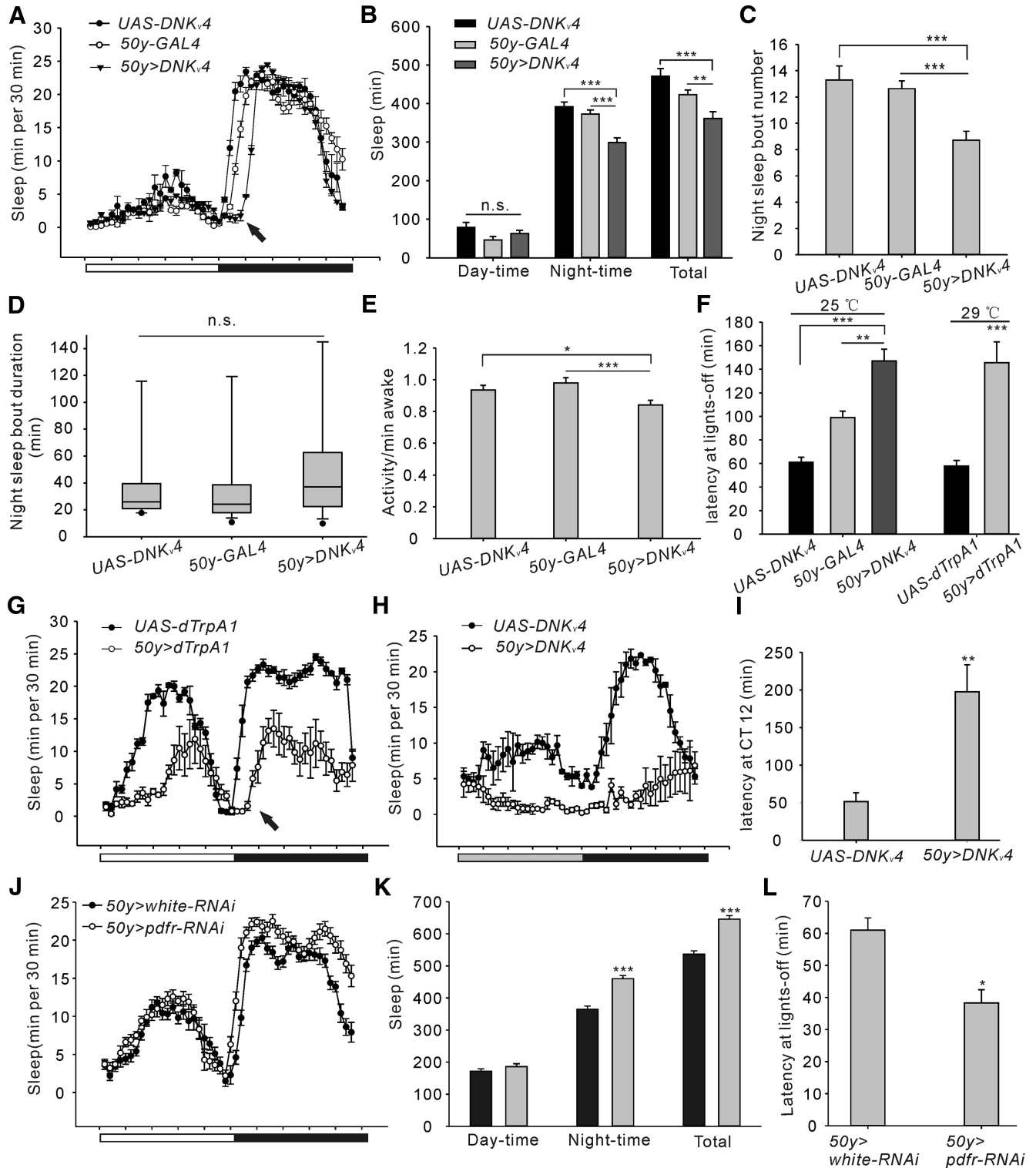


Figure 7. Function-loss of K_v4 in PI also leads to delayed sleep onset. **A**, Conventional sleep plots of controls (*UAS-DNK.4*, *n* = 27; *50y-GAL4*, *n* = 32) and experimental (*50y>DNK.4*, *n* = 49) flies in LD. White and black bars indicate 12 h light/dark periods, respectively, and the arrow indicates delayed sleep onset in experimental flies. **B–E**, Quantification of sleep parameters showing total sleep amount (24 h), sleep during daytime and night-time (**B**), night-time sleep bout number (**C**), night-time sleep duration (**D**), and waking activity (**E**). **F**, Sleep latency after lights-off at ZT12 for controls versus experimental flies at 25°C (left), and *UAS-dTrpA1* vs. *50y>dTrpA1* at 29°C (right). The arrows indicate delayed sleep onset in experimental flies. Quantifications are shown in **F**. **H**, Conventional sleep plots in DD of control (*UAS-DNK.4*, *n* = 30) and experimental (*50y>DNK.4*, *n* = 25) flies. Gray and black bars indicate 12 h subjective day and night, respectively. **I**, Quantification of sleep latency at subjective night in DD for the genotypes as indicated in **H**. **J**, Conventional sleep plots of control (*50y>white-RNAi*, *n* = 26) and experimental (*50y>pdfR-RNAi*, *n* = 28) flies. **K**, **L**, Quantification of sleep amount (**K**) and sleep latency (**L**) for the genotypes as indicated in **J**. Mean ± SEM is shown. **p* < 0.05, ***p* < 0.01, ****p* < 0.001; n.s., not significant. Data are compared by Student's *t* test, except Mann–Whitney *U* test for comparison of nonparametrically distributed data. For multiple comparisons, one-way ANOVAs followed by *post hoc* Tukey were performed. For the quantification of sleep onset in males, see Figure 7-1 (available at <https://doi.org/10.1523/JNEUROSCI.0777-18.2018.f7-1>).

incident with membrane excitability and RMPs oscillations in l-LNVs, but with slight (~1–2 h) delay in peaks (Cao and Nitabach, 2008; Liang et al., 2016). In this study, DNK_v4 preferentially reduced excitability at dusk without causing daily excitability oscillation shifts (Fig. 5F), and presumably would reduce Ca²⁺ peaks as well. But how K_v4 exactly regulates intracellular Ca²⁺ waves and coordination of electrical excitability and Ca²⁺ waves need further study.

PI exerts its effects as downstream of clock neurons and is one of the key targets (direct or indirect) of PDF neurons, although PI cells do not express molecular clock machinery (Jaramillo et al., 2004; Chung et al., 2009; Cavanaugh et al., 2014). Previous studies have suggested that EGFR/ERK signal in insulin-producing PI neurons plays important roles in regulating the consolidation and maintenance of sleep in *Drosophila*, indicating that PI cells act as wake-promoting neurons (Foltenyi et al., 2007; Cong et al., 2015; Barber et al., 2016). Our results are the first to demonstrate that the neuronal activities and PDF/PDFR signaling in subsets of PI cells (*50y-GAL4* driver) participate in the regulation of sleep onset.

In this study, defects in sleep initiation were presumed to be due to the hyperactivity of specific circadian neurons caused by blocking K_v4 activity. dTrpA1 experiments further supported this notion. However, a recent study concluded that reducing the Shaker/K_v1 current would decrease, rather than increase, the action potential discharge in dFB (dorsal FB; Pimentel et al., 2016). Depleting Shaker from dFB neurons could shift the interspike interval distribution toward longer values, making it more difficult to generate next spike. We suppose that the opposite effect may be due to diverse types of K_v channels and different discharge and biophysical properties of neurons. For example, K_v4 is required for maintaining excitability in cultured neurons (Ping et al., 2011), but not in groups of neurons from dissected brain in this study (Figs. 4, 5). Whether driving DNK_v4 expression in other sleep-promoting or wake-promoting neurons would cause parallel or opposite effects on sleep needs to be investigated. Neurons in EB (Liu et al., 2016), FB (Donlea et al., 2014; Pimentel et al., 2016), or a subset MBNs driven by *201y-GAL4* (Cavanaugh et al., 2016) could be tested in further studies.

Previous work has provided a strong link between circadian periods with habitual sleep timing in human, and *CRY1* is suggested to be associated with a familial form of delayed sleep phase disorder (Wright et al., 2005; Patke et al., 2017). However, we did not detect significant change in circadian periods by blocking K_v4 in LNVs and DN1s, indicating that delayed sleep onset in the mutants was not due to changes in circadian periods. Blocking K_v4 in PI cells disrupted rhythmic activities in most flies and we did detect a lengthened circadian period in the rhythmic ones. Because PI is a circadian output region and does not express clock machinery, it is not likely that intrinsic circadian rhythm disorder contributes to the sleep onset phenotype caused by blocking K_v4.

Studies have provided evidence that links types of potassium channels to sleep phenotypes in *Drosophila* and human (Cornelius et al., 2011; Allebrandt et al., 2013; Barone and Krieger, 2016). For example, insomnia has been delineated in patients with neurologic disorders of Voltage-gated K⁺ channels (K_v) autoimmunity (or named K_v antibody syndrome). Sleep onset insomnia, defined as inability to fall asleep at the desired time, is observed in patients with neurodegenerative diseases and psychiatric disorders (Wulff et al., 2010). Abnormal sleep timing and pattern have also been observed in *Drosophila* disease models (Wulff et al., 2010; Tabuchi et al., 2015; Gonzales et al., 2016; Song et al., 2017).

Our study may provide a potential alternative therapy of sleep onset insomnia by targeting K_v4 channels.

References

- Afonso DJ, Liu D, Machado DR, Pan H, Jepson JE, Rogulja D, Koh K (2015) TARANIS functions with cyclin A and Cdk1 in a novel arousal center to control sleep in *Drosophila*. *Curr Biol* 25:1717–1726. [CrossRef Medline](#)
- Agosto J, Choi JC, Parisky KM, Stilwell G, Rosbash M, Griffith LC (2008) Modulation of GABAA receptor desensitization uncouples sleep onset and maintenance in *Drosophila*. *Nat Neurosci* 11:354–359. [CrossRef Medline](#)
- Allebrandt KV, Amin N, Müller-Myhsok B, Esko T, Teder-Laving M, Azevedo RV, Hayward C, van Mill J, Vogelzangs N, Green EW, Melville SA, Lichtner P, Wichmann HE, Oostra BA, Janssens AC, Campbell H, Wilson JF, Hicks AA, Pramstaller PP, Dogas Z, et al. (2013) A K(ATP) channel gene effect on sleep duration: from genome-wide association studies to function in *Drosophila*. *Mol Psychiatry* 18:122–132. [CrossRef Medline](#)
- Artiushin G, Sehgal A (2017) The *Drosophila* circuitry of sleep–wake regulation. *Curr Opin Neurobiol* 44:243–250. [CrossRef Medline](#)
- Barber AF, Erion R, Holmes TC, Sehgal A (2016) Circadian and feeding cues integrate to drive rhythms of physiology in *Drosophila* insulin-producing cells. *Genes Dev* 30:2596–2606. [CrossRef Medline](#)
- Barone DA, Krieger AC (2016) Sleep disturbances in voltage-gated potassium channel antibody syndrome. *Sleep Med* 21:171–173. [CrossRef Medline](#)
- Bergquist S, Dickman DK, Davis GW (2010) A hierarchy of cell intrinsic and target-derived homeostatic signaling. *Neuron* 66:220–234. [CrossRef Medline](#)
- Cao G, Nitabach MN (2008) Circadian control of membrane excitability in *Drosophila melanogaster* lateral ventral clock neurons. *J Neurosci* 28:6493–6501. [CrossRef Medline](#)
- Cavanaugh DJ, Geratowski JD, Wooltorton JR, Spaethling JM, Hector CE, Zheng X, Johnson EC, Eberwine JH, Sehgal A (2014) Identification of a circadian output circuit for rest:activity rhythms in *Drosophila*. *Cell* 157:689–701. [CrossRef Medline](#)
- Cavanaugh DJ, Vigderman AS, Dean T, Garbe DS, Sehgal A (2016) The *Drosophila* circadian clock gates sleep through time-of-day dependent modulation of sleep-promoting neurons. *Sleep* 39:345–356. [CrossRef Medline](#)
- Cavey M, Collins B, Bertet C, Blau J (2016) Circadian rhythms in neuronal activity propagate through output circuits. *Nat Neurosci* 19:587–595. [CrossRef Medline](#)
- Chung BY, Kilman VL, Keath JR, Pitman JL, Allada R (2009) The GABA(A) receptor RDL acts in peptidergic PDF neurons to promote sleep in *Drosophila*. *Curr Biol* 19:386–390. [CrossRef Medline](#)
- Cirelli C, Bushey D, Hill S, Huber R, Kreber R, Ganetzky B, Tononi G (2005) Reduced sleep in *Drosophila* shaker mutants. *Nature* 434:1087–1092. [CrossRef Medline](#)
- Colwell CS (2011) Linking neural activity and molecular oscillations in the SCN. *Nat Rev Neurosci* 12:553–569. [CrossRef Medline](#)
- Cong X, Wang H, Liu Z, He C, An C, Zhao Z (2015) Regulation of sleep by insulin-like peptide system in *Drosophila melanogaster*. *Sleep* 38:1075–1083. [CrossRef Medline](#)
- Cornelius JR, Pittock SJ, McKeon A, Lennon VA, Aston PA, Josephs KA, Tippmann-Peikert M, Silber MH (2011) Sleep manifestations of voltage-gated potassium channel complex autoimmunity. *Arch Neurol* 68:733–738. [CrossRef Medline](#)
- Covarrubias M, Wei AA, Salkoff L (1991) Shaker, Shal, Shab, and Shaw express independent K⁺ current systems. *Neuron* 7:763–773. [CrossRef Medline](#)
- Crocker A, Shahidullah M, Levitan IB, Sehgal A (2010) Identification of a neural circuit that underlies the effects of octopamine on sleep:wake behavior. *Neuron* 65:670–681. [CrossRef Medline](#)
- Depetris-Chauvin A, Berni J, Aranovich EJ, Muraro NI, Beckwith EJ, Ceriani MF (2011) Adult-specific electrical silencing of pacemaker neurons uncouples molecular clock from circadian outputs. *Curr Biol* 21:1783–1793. [CrossRef Medline](#)
- de Velasco B, Erclik T, Shy D, Sclafani J, Lipshitz H, McInnes R, Hartenstein V (2007) Specification and development of the pars intercerebralis and pars lateralis, neuroendocrine command centers in the *Drosophila* brain. *Dev Biol* 302:309–323. [CrossRef Medline](#)

- Diao F, Chaufty J, Waro G, Tsunoda S (2010) SIDL interacts with the dendritic targeting motif of shal (K(v)4) K⁺ channels in *Drosophila*. *Mol Cell Neurosci* 45:75–83. [CrossRef Medline](#)
- Donlea JM, Pimentel D, Miesenböck G (2014) Neuronal machinery of sleep homeostasis in *Drosophila*. *Neuron* 81:860–872. [CrossRef Medline](#)
- Douglas CL, Vyazovskiy V, Southard T, Chiu SY, Messing A, Tonomi G, Cirelli C (2007) Sleep in Kcna2 knockout mice. *BMC Biol* 5:42. [CrossRef Medline](#)
- Dubowy C, Sehgal A (2017) Circadian rhythms and sleep in *Drosophila melanogaster*. *Genetics* 205:1373–1397. [CrossRef Medline](#)
- Feng G, Pang J, Yi X, Song Q, Zhang J, Li C, He G, Ping Y (2018) Downregulation of KV4 channel in *Drosophila* mushroom body neurons contributes to Abeta42-induced courtship memory deficits. *Neuroscience* 370:236–245. [CrossRef Medline](#)
- Foltenyi K, Greenspan RJ, Newport JW (2007) Activation of EGFR and ERK by rhomboid signaling regulates the consolidation and maintenance of sleep in *Drosophila*. *Nat Neurosci* 10:1160–1167. [CrossRef Medline](#)
- Gasque G, Labarca P, Reynaud E, Darszon A (2005) Shal and shaker differential contribution to the K⁺ currents in the *Drosophila* mushroom body neurons. *J Neurosci* 25:2348–2358. [CrossRef Medline](#)
- Gonzales ED, Tanenhaus AK, Zhang J, Chaffee RP, Yin JC (2016) Early-onset sleep defects in *Drosophila* models of Huntington's disease reflect alterations of PKA/CREB signaling. *Hum Mol Genet* 25:837–852. [CrossRef Medline](#)
- Granados-Fuentes D, Norris AJ, Carrasquillo Y, Nerbonne JM, Herzog ED (2012) *I_A* channels encoded by Kv1.4 and Kv4.2 regulate neuronal firing in the suprachiasmatic nucleus and circadian rhythms in locomotor activity. *J Neurosci* 32:10045–10052. [CrossRef Medline](#)
- Guo F, Yu J, Jung HJ, Abruzzi KC, Luo W, Griffith LC, Rosbash M (2016) Circadian neuron feedback controls the *Drosophila* sleep–activity profile. *Nature* 536:292–297. [CrossRef Medline](#)
- Im SH, Taghert PH (2010) PDF receptor expression reveals direct interactions between circadian oscillators in *Drosophila*. *J Comp Neurol* 518:1925–1945. [CrossRef Medline](#)
- Jaramillo AM, Zheng X, Zhou Y, Amado DA, Sheldon A, Sehgal A, Levitan IB (2004) Pattern of distribution and cycling of SLOB, Slowpoke channel binding protein, in *Drosophila*. *BMC Neurosci* 5:3. [CrossRef Medline](#)
- Joiner WJ, Crocker A, White BH, Sehgal A (2006) Sleep in *Drosophila* is regulated by adult mushroom bodies. *Nature* 441:757–760. [CrossRef Medline](#)
- Kayser MS, Biron D (2016) Sleep and development in genetically tractable model organisms. *Genetics* 203:21–33. [CrossRef Medline](#)
- Keene AC, Duboué ER, McDonald DM, Dus M, Suh GS, Waddell S, Blau J (2010) Clock and cycle limit starvation-induced sleep loss in *Drosophila*. *Curr Biol* 20:1209–1215. [CrossRef Medline](#)
- Kunst M, Hughes ME, Raccuglia D, Felix M, Li M, Barnett G, Duah J, Nitabach MN (2014) Calcitonin gene-related peptide neurons mediate sleep-specific circadian output in *Drosophila*. *Curr Biol* 24:2652–2664. [CrossRef Medline](#)
- Liang X, Holy TE, Taghert PH (2016) Synchronous *Drosophila* circadian pacemakers display nonsynchronous Ca²⁺ rhythms *in vivo*. *Science* 351:976–981. [CrossRef Medline](#)
- Li Q, Li Y, Wang X, Qi J, Jin X, Tong H, Zhou Z, Zhang ZC, Han J (2017) Fbxl4 serves as a clock output molecule that regulates sleep through promotion of rhythmic degradation of the GABA_A receptor. *Curr Biol* 27:3616–3625.e5. [CrossRef Medline](#)
- Liu S, Lamaze A, Liu Q, Tabuchi M, Yang Y, Fowler M, Bharadwaj R, Zhang J, Bedont J, Blackshaw S, Lloyd TE, Montell C, Sehgal A, Koh K, Wu MN (2014) WIDE AWAKE mediates the circadian timing of sleep onset. *Neuron* 82:151–166. [CrossRef Medline](#)
- Liu S, Liu Q, Tabuchi M, Wu MN (2016) Sleep drive is encoded by neural plastic changes in a dedicated circuit. *Cell* 165:1347–1360. [CrossRef Medline](#)
- Liu W, Guo F, Lu B, Guo A (2008) amnesiac regulates sleep onset and maintenance in *Drosophila melanogaster*. *Biochem Biophys Res Commun* 372:798–803. [CrossRef Medline](#)
- Parisky KM, Agosto J, Pulver SR, Shang Y, Kuklin E, Hodge JJ, Kang K, Liu X, Garrity PA, Rosbash M, Griffith LC (2008) PDF cells are a GABA-responsive wake-promoting component of the *Drosophila* sleep circuit. *Neuron* 60:672–682. [CrossRef Medline](#)
- Park S, Sonn JY, Oh Y, Lim C, Choe J (2014) SIFamide and SIFamide receptor defines a novel neuropeptide signaling to promote sleep in *Drosophila*. *Mol Cells* 37:295–301. [CrossRef Medline](#)
- Parrish JZ, Kim CC, Tang L, Bergquist S, Wang T, Derisi JL, Jan LY, Jan YN, Davis GW (2014) Kruppel mediates the selective rebalancing of ion channel expression. *Neuron* 82:537–544. [CrossRef Medline](#)
- Patke A, Murphy PJ, Onat OE, Krieger AC, Özçelik T, Campbell SS, Young MW (2017) Mutation of the human circadian clock gene *CRY1* in familial delayed sleep phase disorder. *Cell* 169:203–215.e13. [CrossRef Medline](#)
- Pimentel D, Donlea JM, Talbot CB, Song SM, Thurston AJ, Miesenböck G (2016) Operation of a homeostatic sleep switch. *Nature* 536:333–337. [CrossRef Medline](#)
- Ping Y, Tsunoda S (2011) Inactivity-induced increase in nAChRs upregulates shal K(+) channels to stabilize synaptic potentials. *Nat Neurosci* 15:90–97. [CrossRef Medline](#)
- Ping Y, Waro G, Licursi A, Smith S, Vo-Ba DA, Tsunoda S (2011) Shal/K(v)4 channels are required for maintaining excitability during repetitive firing and normal locomotion in *Drosophila*. *PLoS One* 6:e16043. [CrossRef Medline](#)
- Ping Y, Hahm ET, Waro G, Song Q, Vo-Ba DA, Licursi A, Bao H, Ganoe L, Finch K, Tsunoda S (2015) Linking Aβ42-induced hyperexcitability to neurodegeneration, learning and motor deficits, and a shorter lifespan in an Alzheimer's model. *PLoS Genet* 11:e1005025. [CrossRef Medline](#)
- Pitman JL, McGill JJ, Keegan KP, Allada R (2006) A dynamic role for the mushroom bodies in promoting sleep in *Drosophila*. *Nature* 441:753–756. [CrossRef Medline](#)
- Rogero O, Hämmerle B, Tejedor FJ (1997) Diverse expression and distribution of shaker potassium channels during the development of the *Drosophila* nervous system. *J Neurosci* 17:5108–5118. [CrossRef Medline](#)
- Rogulja D, Young MW (2012) Control of sleep by cyclin A and its regulator. *Science* 335:1617–1621. [CrossRef Medline](#)
- Rosenberg RP (2006) Sleep maintenance insomnia: strengths and weaknesses of current pharmacologic therapies. *Ann Clin Psychiatry* 18:49–56. [CrossRef Medline](#)
- Salkoff L, Wyman R (1981) Genetic modification of potassium channels in *Drosophila* shaker mutants. *Nature* 293:228–230. [CrossRef Medline](#)
- Shang Y, Griffith LC, Rosbash M (2008) Light-arousal and circadian photo-reception circuits intersect at the large PDF cells of the *Drosophila* brain. *Proc Natl Acad Sci U S A* 105:19587–19594. [CrossRef Medline](#)
- Sheeba V, Fogle KJ, Kaneko M, Rashid S, Chou YT, Sharma VK, Holmes TC (2008a) Large ventral lateral neurons modulate arousal and sleep in *Drosophila*. *Curr Biol* 18:1537–1545. [CrossRef Medline](#)
- Sheeba V, Gu H, Sharma VK, O'Dowd DK, Holmes TC (2008b) Circadian- and light-dependent regulation of resting membrane potential and spontaneous action potential firing of *Drosophila* circadian pacemaker neurons. *J Neurophysiol* 99:976–988. [CrossRef Medline](#)
- Song Q, Feng G, Huang Z, Chen X, Chen Z, Ping Y (2017) Aberrant axonal arborization of PDF neurons induced by Abeta42-mediated JNK activation underlies sleep disturbance in an Alzheimer's model. *Mol Neurobiol* 54:6317–6328. [CrossRef Medline](#)
- Srinivasan S, Lance K, Levine RB (2012) Segmental differences in firing properties and potassium currents in *Drosophila* larval motoneurons. *J Neurophysiol* 107:1356–1365. [CrossRef Medline](#)
- Stoleru D, Peng Y, Agosto J, Rosbash M (2004) Coupled oscillators control morning and evening locomotor behaviour of *Drosophila*. *Nature* 431:862–868. [CrossRef Medline](#)
- Strauss R, Heisenberg M (1993) A higher control center of locomotor behavior in the *Drosophila* brain. *J Neurosci* 13:1852–1861. [CrossRef Medline](#)
- Tabuchi M, Lone SR, Liu S, Liu Q, Zhang J, Spira AP, Wu MN (2015) Sleep interacts with Aβ to modulate intrinsic neuronal excitability. *Curr Biol* 25:702–712. [CrossRef Medline](#)
- Ueda A, Wu CF (2006) Distinct frequency-dependent regulation of nerve terminal excitability and synaptic transmission by *I_A* and *I_K* potassium channels revealed by *Drosophila Shaker* and *Shab* mutations. *J Neurosci* 26:6238–6248. [CrossRef Medline](#)
- Wei A, Covarrubias M, Butler A, Baker K, Pak M, Salkoff L (1990) K⁺ current diversity is produced by an extended gene family conserved in *Drosophila* and mouse. *Science* 248:599–603. [CrossRef Medline](#)
- Wright KP Jr, Gronfier C, Duffy JF, Czeisler CA (2005) Intrinsic period and light intensity determine the phase relationship between melatonin and sleep in humans. *J Biol Rhythms* 20:168–177. [CrossRef Medline](#)
- Wulff K, Gatti S, Wettstein JG, Foster RG (2010) Sleep and circadian rhythm disruption in psychiatric and neurodegenerative disease. *Nat Rev Neurosci* 11:589–599. [CrossRef Medline](#)